

A Novel Proton Decay Signature at DUNE, JUNO, and Hyper-K

Florian Domingo,^a Herbi K. Dreiner,^a Dominik Köhler,^a Saurabh Nangia,^a and Apoorva Shah^a

^a*Bethe Center for Theoretical Physics & Physikalisches Institut der Universität Bonn, Nußallee 12, 53115 Bonn, Germany*

E-mail: domingo@physik.uni-bonn.de, dreiner@uni-bonn.de,
koehler@physik.uni-bonn.de, nangia@physik.uni-bonn.de,
ashah@uni-bonn.de

ABSTRACT:

Proton decay, although unobserved so far, is a natural expectation when attempting to explain the baryon asymmetry of the universe. $p \rightarrow K^+ \bar{\nu}$ or $p \rightarrow K^+ \tilde{\chi}_1^0$, with $\tilde{\chi}_1^0$ a light exotic neutral particle, represent possible decay channels achievable in models of physics beyond the Standard Model, such as the MSSM with trilinear R-parity-violating terms, or the Standard Model extended by a heavy neutral lepton. Among the decay products of these modes, the neutral fermions would typically appear as missing energy in collider searches. The present study considers how such decay modes could be differentiated in experimental settings, as the exotic $\tilde{\chi}_1^0$ may further decay if it is not protected by a symmetry (such as R-parity in the MSSM). We assess the detection prospects of the proposed experiments DUNE, JUNO and Hyper-K in this context.

Contents

1	Introduction	1
2	The Signature: Proton Decay followed by Neutralino Decay	3
2.1	Proton Decay to a light Neutralino in the RPV-MSSM	3
2.2	Neutralino Decay	7
3	Proton Decay Experiments	9
3.1	Detectors	9
3.2	Prospects for the Detection of the Neutralino Final State	10
3.3	Proton Decay in Nuclei	11
3.4	Simulation Procedure	13
4	Numerical Analysis	15
4.1	Benchmark Scenarios	16
4.2	Results	17
5	Conclusions	22
A	Heavy Neutral Lepton	23

1 Introduction

Despite its many successes, the Standard Model (SM) of particle physics cannot be viewed as an exhaustive description of Nature. One of the essential puzzles from the cosmological perspective is embodied by the prevalence of matter over antimatter in the observable Universe [1, 2]. Baryogenesis [3] appears as a viable explanation of this obvious discrepancy between SM and observations, provided that baryon number (B), in particular, is violated in particle interactions. In the SM, this quantity is accidentally conserved at the perturbative level, along with lepton number (L); here, ‘accidental’ means that the most general renormalizable gauge-invariant (perturbative) interactions automatically preserve these quantum numbers. Violation of the baryon number through non-perturbative effects in the SM, such as instantons and sphalerons [4–7], proves insufficient to account for the observed asymmetry [8–11].

Still, theoretical frameworks extending beyond the SM, such as Grand Unified Theories (GUTs) [12], supersymmetry (SUSY) [13–19], or theories of quantum gravity [20, 21], can effortlessly provide new sources of baryon-number violation (or of lepton-number violation when considering the leptogenesis mechanism [22–25]). However, a drastic consequence of introducing such effects is the simultaneous emergence of proton decay [26–29],

the latter remaining unobserved to this date, with the current strongest bound on the lifetime $\tau(p \rightarrow \pi^0 + e^+) > 1.6 \times 10^{34}$ yrs [30]. Nevertheless, the host of upcoming next-generation detectors under construction or planned, such as DUNE [31–34], JUNO [35, 36], and Hyper-K [37], will certainly help shed a new light on the hypothetical proton instability, and we believe it essential, on the phenomenological side, to point at possible decay signatures that would be overlooked in the traditional approach.

In this paper, we focus on a proton disintegration dominated by kaons in the final states, with modes such as $p \rightarrow K^+ \bar{\nu}$ and $p \rightarrow K^+ \tilde{\chi}_1^0$, where $\tilde{\chi}_1^0$ is a light exotic neutral particle with

$$m_{\tilde{\chi}_1^0} \leq m_p - m_{K^+} \approx 445 \text{ MeV}. \quad (1.1)$$

This scenario can be easily embedded within the phenomenology of the Minimal Supersymmetric Standard Model with R-parity-violating terms (RPV-MSSM), and we shall employ this model as a predictive framework for our study. However, one could also consider instead the decay to a heavy neutral lepton (N_R): $p \rightarrow K^+ N_R$, see our Appendix A, and for example Ref. [38].

Originally motivated by the Hierarchy Problem [39, 40], SUSY extensions of the SM [13] have far-reaching phenomenological consequences at low-energy, with features such as dark matter candidates, gauge-coupling unification, or neutrino-mass generation. We refer the reader to e.g. Refs. [16, 18, 41] for an overview. In contrast to the SM, baryon- and lepton-number violating interactions are naturally present in these models at the renormalizable level, unless an additional discrete symmetry, often (but not imperatively) R-parity [42], is explicitly requested [18, 26, 43, 44]. There exists no deep theoretical motivation to exclude such terms via R-parity [45–47], but experimental evidence for a generally B- and L-conserving phenomenology at low-energy implies that they remain comparatively suppressed. In particular, they may trigger proton decay, which is the feature in which we are interested here. Nevertheless, we stress that R-parity conservation does not forbid B- and L-violation in higher-order operators, so that proton instability can also be expected in the R-parity conserving MSSM when the latter is considered as an effective field theory [26, 45, 48].

Numerous aspects of proton disintegration in the RPV-MSSM have been studied in the literature in the past: the reader may consult e.g. Refs. [41, 49–51]. Two-body final states with only SM particles imply a violation of both B and L: spin-conservation indeed dictates the presence of an odd number of fermions among the decay products and, in the SM, these can only be leptons, then produced in association with a meson. Sfermions mediate such processes at tree-level in the RPV-MSSM [52, 53], provided both B- and L-violating couplings are simultaneously present. More involved topologies have also been considered [54–58], leading to bounds on a wide set of products of RPV couplings. Nevertheless, proton disintegration involving only B-violation is a viable scenario as well, as long as a light exotic fermion $\tilde{\chi}_1^0$ is available in the spectrum. In particular, the cases involving a light photino [54, 59], a light gravitino or axino [60, 61] have been considered in the literature. In this paper, we identify $\tilde{\chi}_1^0$ with the lightest, bino-like neutralino, which is the only phenomenologically viable candidate within the strict limits of the MSSM spectrum.

A low-mass particle of this nature indeed evades existing experimental constraints [62, 63]. Astrophysical constraints are also satisfied [64, 65]. Cosmological and astrophysical limits however demand that it is unstable, which, in view of the mass and suppressed couplings of this particle, typically makes it long-lived. We assume that the bino decays are dominated by L-violating channels, triggering final states with leptons and mesons. More exotic decay channels involving e.g. axinos or gravitinos are an alternative. Searches of the light neutralino at colliders have been recently proposed in [66–72], in the more general context of searches for long-lived particles [73–79].

$p \rightarrow K^+ \tilde{\chi}_1^0$ appears as the simplest proton decay mode violating only B in the context of the RPV-MSSM. On a superficial level, it shares many similarities with the canonical mode $p \rightarrow K^+ \bar{\nu}$, for which **Super-Kamiokande** provides the (currently strictest) limit $\tau_{p \rightarrow K^+ \bar{\nu}} > 5.9 \times 10^{33}$ yrs [80]. The light long-lived bino might distinguish itself from the neutrino through its mass, reducing the kaon momentum in experiments. In addition, for decay lengths comparable to the detector size, the neutralino could decay within the detector, leading to a distinct signature. We analyze both possibilities in detail and reinterpret the **Super-K** bound in this context. We also calculate the sensitivities of the upcoming experiments **DUNE**, **JUNO**, and **Hyper-K** to such a proton-decay mode.

The paper is organized as follows: in Section 2, we introduce the RPV-MSSM, as well as the light-neutralino scenario. We discuss proton decay modes in such a setup, including the resulting signatures. In Section 3, we briefly discuss the experimental setups at present and upcoming proton-decay search facilities: **Super-K** [81], **Hyper-K**, **DUNE** and **JUNO**. We further discuss the prospects for detecting a light exotic fermion, such as a neutralino in these detectors, as well as what happens when a proton decays inside a nucleus with large mass number A . We conclude this section with a description of our simulation procedure for estimating the sensitivities at the above experiments. In Section 4, we outline our numerical analysis and present our results. We conclude in Section 5. In Appendix A, we discuss the close connection between the light neutralino we have discussed extensively here and the related heavy neutral lepton scenario.

2 The Signature: Proton Decay followed by Neutralino Decay

We first discuss the decay of the proton in our model and subsequently the various decays of the light neutralino.

2.1 Proton Decay to a light Neutralino in the RPV-MSSM

As explained in the introduction, we work, for convenience, within the framework of the RPV-MSSM model with a light neutralino. The renormalizable superpotential may be expressed in the notation of Ref. [44]:

$$W = W_{\text{MSSM}} + W_{\text{LNV}} + W_{\text{BNV}}, \quad (2.1)$$

where W_{MSSM} is the MSSM superpotential, and

$$W_{\text{LNV}} = \epsilon_{ab} \left(\frac{1}{2} \lambda_{ijk} L^{ai} L^{bj} \bar{E}^k + \lambda'_{ijk} L^{ai} Q^{bj} \bar{D}^k \right), \quad (2.2)$$

$$W_{\text{BNV}} = \frac{1}{2} \varepsilon_{\alpha\beta\gamma} \lambda''_{ijk} \bar{U}^{\alpha i} \bar{D}^{\beta j} \bar{D}^{\gamma k}, \quad (2.3)$$

violate lepton- and baryon-number, respectively. In W_{LNV} we have dropped the bilinear term, as it can be rotated away at a fixed energy scale [54, 82]. ϵ_{ab} is the two-dimensional Levi-Civita symbol, and the Latin indices $a, b \in \{1, 2\}$ are the $\text{SU}(2)_L$ gauge indices in the fundamental representation. $\varepsilon_{\alpha\beta\gamma}$ is the three-dimensional Levi-Civita symbol and the Greek indices α, β , and $\gamma \in \{1, 2, 3\}$ denote the $\text{SU}(3)_C$ gauge color indices. λ''_{ijk} is a dimensionless Yukawa coupling and $i, j, k \in \{1, 2, 3\}$ denote the generation indices. We employ the summation convention. L^i and Q^i are the $\text{SU}(2)$ -doublet lepton and quark chiral superfields; \bar{E}^i , \bar{U}^i , and \bar{D}^i are $\text{SU}(2)$ -singlet electron-, up- and down-type quark chiral superfields, respectively.

The bino, which we will consider further below, is the spin-1/2 SUSY partner of the hypercharge gauge field. As such, its coupling to matter are dictated by the gauge interaction. As reminded in the introduction, such a particle might exist with an almost arbitrarily low mass without violating collider, astrophysical and cosmological constraints, as long as it is unstable.

In the RPV-MSSM, as well as in any viable model of new physics, B- (and L-) violation manifests itself at low-energy (the proton mass-scale) through the mediation of high-energy fields (taking mass at the SUSY-breaking scale, comparable to or larger than the electroweak scale). In such configurations with a sizable hierarchy of scales, it is always desirable to disentangle long- and short-distance effects through the definition of a low-energy effective field theory (EFT), allowing for the resummation of large logarithmic corrections. The impact of new-physics for low-energy particles is then summarized within contributions to operators of higher-dimension built out of the light fields. The operators of lowest dimension relevant for nucleon decay are of dimension 6: we refer the reader to Ref. [51] for a recent overview of this specific EFT and associated calculation techniques.

The operators that are relevant for the production of a neutral $\text{SU}(2)_L$ -singlet fermion $\tilde{\chi}_1^0$ (*i.e.* neglecting contributions that require an electroweak vacuum expectation value, which receive further mass-suppression from new-physics) read:

$$\begin{aligned} \hat{Q}'_1 &= \varepsilon_{\alpha\beta\gamma} [(\bar{d}^c)^\alpha P_R u^\beta] [(\bar{s}^c)^\gamma P_R \tilde{\chi}_1^{0c}], \\ \hat{Q}_1 &= \varepsilon_{\alpha\beta\gamma} [(\bar{s}^c)^\alpha P_R u^\beta] [(\bar{d}^c)^\gamma P_R \tilde{\chi}_1^{0c}], \\ \hat{Q}_2 &= \varepsilon_{\alpha\beta\gamma} [(\bar{s}^c)^\alpha P_R d^\beta] [(\bar{u}^c)^\gamma P_R \tilde{\chi}_1^{0c}], \end{aligned} \quad (2.4)$$

where P_R is the right-handed projection operator. u, d, s are the four-component quark spinors with c denoting charge conjugation. $\tilde{\chi}_1^0$ denotes the 4-component neutralino spinor, or any other exotic neutral fermion.

Contributions to the operators of Eq.(2.4) emerge at tree-level in the RPV-MSSM through the mediation of a squark, provided a B-violating trilinear coupling $\lambda''_{112} = -\lambda''_{121}$ is

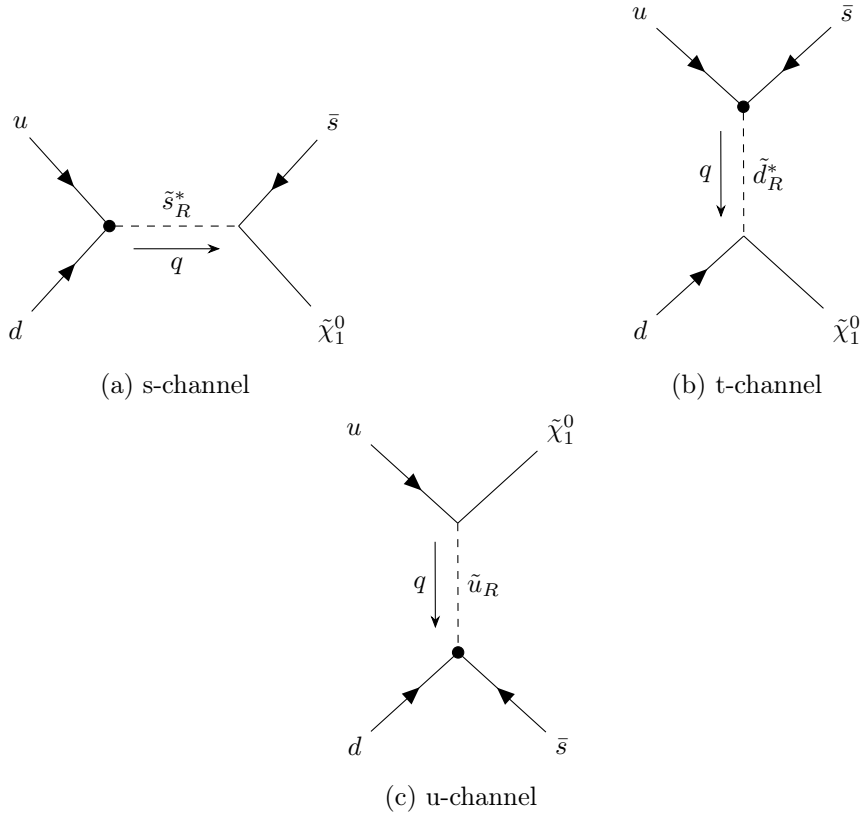


Figure 1: Feynman diagrams depicting the contributions to the four-fermion operators, which in turn contribute to proton decay. The solid black circle shows the RPV vertex.

non-vanishing in the superpotential. The corresponding Wilson coefficients can be obtained by matching of the EFT and read:

$$\begin{aligned}
 C_{\hat{Q}'_1}(\mu_R) &= \eta_{\text{QCD}}(\mu_R) \frac{(-\lambda''_{112}^*)(\sqrt{2}g')}{3m_{\tilde{s}_R}^2}, \\
 C_{\hat{Q}_1}(\mu_R) &= \eta_{\text{QCD}}(\mu_R) \frac{(-\lambda''_{121}^*)(\sqrt{2}g')}{3m_{\tilde{d}_R}^2}, \\
 C_{\hat{Q}_2}(\mu_R) &= \eta_{\text{QCD}}(\mu_R) \frac{(\lambda''_{121}^*)(2\sqrt{2}g')}{3m_{\tilde{u}_R}^2},
 \end{aligned} \tag{2.5}$$

where g' is the $U(1)_Y$ gauge coupling and the masses in the denominator refer to scalar SUSY partners of the right-handed quarks mediating the transition: see Fig.1. $\eta_{\text{QCD}}(\mu_R)$ accounts for the renormalization group evolution of the operators driven by the strong interaction: its expression can be found in Eq.(6) of Ref. [51]. $\eta_{\text{QCD}}(2 \text{ GeV}) \approx 1.4$.

Naturally, the difficult step consists in extracting hadronic matrix elements from these partonic operators. For any operator $\Omega \in \{\hat{Q}_1, \hat{Q}'_1, \hat{Q}_2\}$ of Eq.(2.4), one can derive the

following general form [83] (we employ the $+-$ metric),

$$\begin{aligned}\langle K^+, \tilde{\chi}_1^0(q) | \Omega | p \rangle &= \bar{v}_{\tilde{\chi}_1^0} P_R \left[W_{0,\Omega}^{p \rightarrow K^+}(q^2) - \frac{\not{q}}{m_p} W_{1,\Omega}^{p \rightarrow K^+}(q^2) \right] u_p, \\ &\equiv \bar{v}_{\tilde{\chi}_1^0} P_R \left[W_{\chi,\Omega}^{p \rightarrow K^+}(q^2) \right] u_p,\end{aligned}\quad (2.6)$$

where $W_{0,\Omega}^{p \rightarrow K^+}(q^2)$ and $W_{1,\Omega}^{p \rightarrow K^+}(q^2)$ represent the form factors associated with the operator Ω for the transition $p \rightarrow K^+$, depending on the squared momentum-transfer, q^2 ($= m_{\tilde{\chi}_1^0}^2$ in our case). u_p and $v_{\tilde{\chi}_1^0}$ denote the four-component spinors for the proton and neutralino respectively.

Lattice evaluations of the $p \rightarrow K^+$ form-factors [83–85] focus on the limit $q^2 \rightarrow 0$ (hence on $W_{0,\Omega}^{p \rightarrow K^+}$), corresponding to the neutrino final-state. This limit does not necessarily apply in the case of a neutralino. Alternatively, it is possible to compute the form factors in chiral perturbation theory and determine chiral parameters from the lattice [83], thus retaining full momentum dependence (at leading order in chiral perturbation theory, in practice).

The decay amplitude for the proton decay may now be expressed as follows:

$$\mathcal{A}(p \rightarrow K^+ + \tilde{\chi}_1^0) = i \sum_{\Omega} C_{\Omega} \bar{v}_{\tilde{\chi}_1^0} \left\{ P_R \left[W_{0,\Omega}^{p \rightarrow K^+}(q^2) \right] + P_L \left[\frac{m_{\tilde{\chi}_1^0}}{m_p} W_{1,\Omega}^{p \rightarrow K^+}(q^2) \right] \right\} u_p, \quad (2.7)$$

leading to the partial decay width:

$$\begin{aligned}\Gamma(p \rightarrow K^+ + \tilde{\chi}_1^0) &= \frac{m_p}{32\pi} \left[1 - 2 \frac{m_K^2 + m_{\tilde{\chi}_1^0}^2}{m_p^2} + \left(\frac{m_K^2 - m_{\tilde{\chi}_1^0}^2}{m_p^2} \right)^2 \right]^{1/2} \\ &\left\{ \left(1 + \frac{m_K^2 - m_{\tilde{\chi}_1^0}^2}{m_p^2} \right) \left[\left| \sum_{\Omega} C_{\Omega} W_{0,\Omega}^{p \rightarrow K^+}(m_{\tilde{\chi}_1^0}^2) \right|^2 + \frac{m_{\tilde{\chi}_1^0}^2}{m_p^2} \left| \sum_{\Omega} C_{\Omega} W_{1,\Omega}^{p \rightarrow K^+}(m_{\tilde{\chi}_1^0}^2) \right|^2 \right] \right. \\ &\quad \left. + 4 \frac{m_{\tilde{\chi}_1^0}^2}{m_p^2} \operatorname{Re} \left[\left(\sum_{\Omega} C_{\Omega} W_{0,\Omega}^{p \rightarrow K^+}(m_{\tilde{\chi}_1^0}^2) \right)^* \sum_{\Omega} C_{\Omega} W_{1,\Omega}^{p \rightarrow K^+}(m_{\tilde{\chi}_1^0}^2) \right] \right\}.\end{aligned}\quad (2.8)$$

The decay width normalized to $|\lambda'_{112}|^2/m_{\tilde{f}}^4$, where $m_{\tilde{f}}$ represents a universal value for the squark masses, is shown in Fig. 2 for various lattice inputs. Here, we use the results of the two lattice approaches presented in Refs [84, 85]. The solid lines employ the form-factors retaining full momentum-dependence, while the dashed lines have been obtained under the approximation $W_{\chi,\Omega}^{p \rightarrow K^+}(q^2) \approx W_{\chi,\Omega}^{p \rightarrow K^+}(0)$. The dotted lines account for the quoted lattice uncertainties at 1σ . We observe that the momentum dependence in the form-factors can be neglected in view of the large uncertainty originating in the lattice modelization. Obviously, no better than an order of magnitude can be set on the actual size of the hadronic matrix elements, while the variations due to momentum dependence typically remain under 10%.

Assuming that the neutralinos would behave as an invisible particle at **Super-K**, one may exploit the limit of this experiment for the decay rate $p \rightarrow K^+ \bar{\nu}$. In the massless neutralino limit, this led Ref. [51] to the limit:

$$|\lambda'_{121}|/m_{\tilde{f}}^2 < 3.9 \times 10^{-31} \text{ GeV}^{-2}, \quad (2.9)$$

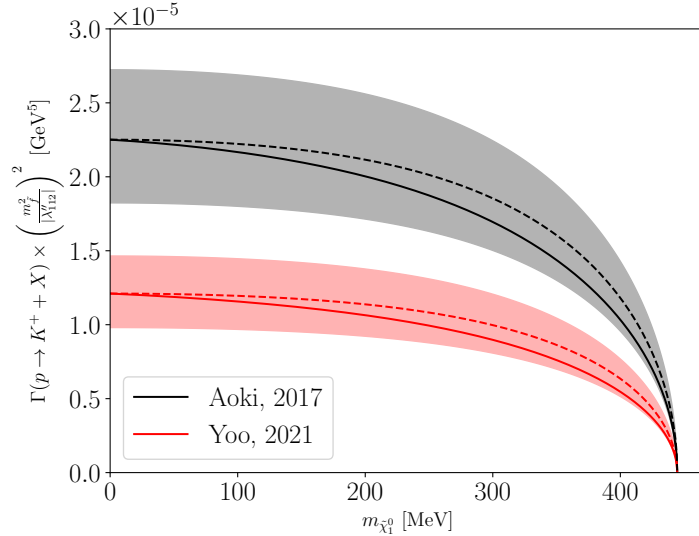


Figure 2: Proton decay width normalised to $|\lambda''_{112}|^2/m_{\tilde{f}}^4$, where $m_{\tilde{f}}$ represents a universal value for the squark masses. Two different lattice evaluations are used for the numerical values of the form factors: from Aoki, 2017 [84] and Yoo, 2021 [85]. The dashed line represents the case where lattice form-factors at $q^2 = 0$ are used, whatever the neutralino mass, while the solid lines represent results with form factors determined according to chiral perturbation theory [83]. The bands around the dashed lines denote the approximate error in the lattice calculation of the form factors.

updating older estimates. This bound can naively be extended to massive neutralinos through a rescaling by the square-root of the quantity depicted in Fig. 2.

Nevertheless, this simplistic picture holds only under the approximation where the modified kaon kinematics (due to the neutralino mass) and subsequent neutralino decays have a negligible impact on the experimental strategy. The purpose of this paper exactly consists in demonstrating how these two effects may leave their imprint on the experimental results, allowing, under favorable conditions, to disentangle the decay mode involving the neutralino from the more classical channels with a(n anti)neutrino in the final state.

Considering the kinematical effect first, we write the kaon momentum in the rest-frame of the proton:

$$|\vec{p}_{K^+}| = \frac{m_p}{2} \sqrt{1 - 2 \frac{m_K^2 + m_{\tilde{\chi}_1^0}^2}{m_p^2} + \left(\frac{m_K^2 - m_{\tilde{\chi}_1^0}^2}{m_p^2} \right)^2}. \quad (2.10)$$

This quantity is shown in Fig. 3. In the massless neutralino limit (or in the case of a neutrino in the final state), $|\vec{p}_{K^+}| \approx 339$ MeV.

2.2 Neutralino Decay

The second experimental handle on the decay channel involving the neutralino rests with the possible observation of neutralino decay products within the detector, which obviously only

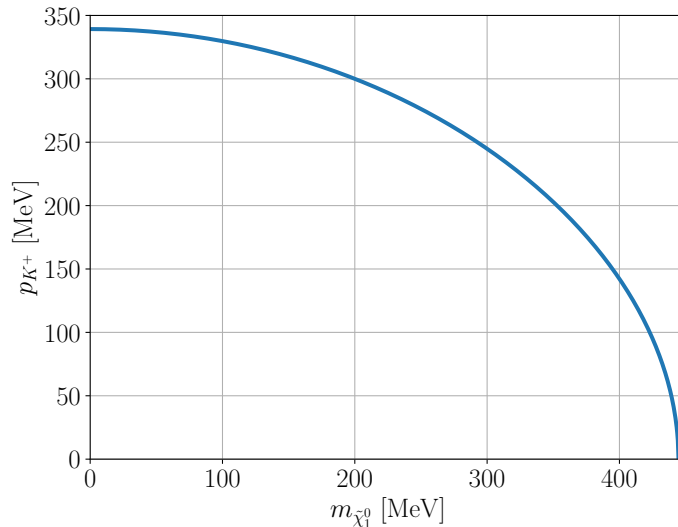


Figure 3: Momentum of the final state kaon as a function of the neutralino mass in the process $p \rightarrow K^+ + \tilde{\chi}_1^0$.

applies if the neutralino is sufficiently short-lived. The decay modes of a light neutralino have been recently reviewed in Ref. [86] and we briefly present the channels relevant for our study. Under the assumption that neutralino decays involving lighter exotic fermions, such as axinos or gravitinos, in the final state are absent or subdominant, neutralino disintegrations necessarily violate lepton number, as the only accessible lighter fermions (needed for the conservation of angular momentum) are muons, electrons or neutrinos. Interactions of this type are possible in the RPV-MSSM, see Eq. (2.2).

The first possibility is that neutralino decays are controlled by $LQ\bar{D}$ operators. Couplings of this type lead to semi-leptonic disintegrations. Considering the mass-regime relevant here, $m_{\tilde{\chi}_1^0} \lesssim 445$ MeV, a pion would be the only kinematically accessible meson. The expressions for the partial decay widths $\Gamma(\tilde{\chi}_1^0 \rightarrow \pi^{\pm/0} + \ell_i^{\mp}/\nu_i)$ in the limit of a pure bino state can be found in Ref. [66]. The RPV couplings involved here (discarding CKM mixing, see [87, 88]) are λ'_{i11} , $i = 1, 2, 3$.¹ In addition, we stress that, with both λ'_{112} and λ'_{i11} non-vanishing, protons may directly employ the decay mode $p \rightarrow K^+ \bar{\nu}_i$ (see e.g. Ref. [51]). For small λ'_{i11} (which is the relevant regime with a long-lived bino), the associated decay width is correspondingly suppressed, however, with respect to the $p \rightarrow K^+ \tilde{\chi}_1^0$ mode (provided the latter is kinematically open). Thus, these two proton decay modes can only compete close to the neutralino production threshold, or for $\lambda'_{i11} \approx 1$.

Purely leptonic decays of the neutralino can be mediated by operators of the $LL\bar{E}$ -type. In the pure bino approximation, neglecting all mixing effects in the sfermion sector

¹Note for the decay $\tilde{\chi}_1^0 \rightarrow \pi^{\pm} + \ell_i^{\mp}$ only $i = 1, 2$ is kinematically possible.

and exploiting $m_{\tilde{\chi}_1^0} \ll m_{\tilde{f}}$, where $m_{\tilde{f}}$ represents a universal sfermion mass, one obtains [89]:

$$\Gamma\left(\tilde{\chi}_1^0 \rightarrow \bar{\nu}_i + \ell_j^+ + \ell_k^-\right) = \frac{3g'^2 |\lambda_{ijk}|^2 m_{\tilde{\chi}_1^0}^5}{2^{12} \pi^3 m_{\tilde{f}}^4}, \quad (i \neq j). \quad (2.11)$$

Finally, both *LQD* and *LLE* operators produce the radiative decays [54, 70, 86, 90, 91],

$$\Gamma(\tilde{\chi}_1^0 \rightarrow \gamma + \nu_i/\bar{\nu}_i) = \frac{\alpha^2 m_{\tilde{\chi}_1^0}^3}{512 \pi^3 \cos^2 \theta_W} |\lambda_{iff}^{(\prime)}|^2 \left[\frac{e_f N_c^f m_f (4e_f + 1)}{m_{\tilde{f}}^2} \left(1 + \log \frac{m_{\tilde{f}}^2}{m_f^2} \right) \right]^2, \quad (2.12)$$

where $\lambda_{iff}^{(\prime)}$ is the relevant trilinear coupling ($L_i Q_j \bar{D}_j$ or $L_i L_j \bar{E}_j$), f/\tilde{f} the associated fermions/sfermions running in the one-loop diagram, e_f their electric charge in units of e , $m_f/m_{\tilde{f}}$ their masses, N_c^f their color number (1 or 3). Once again, simplifying assumptions have been used as to the scalar sector.

Both the tree-level and radiative decay modes can be relevant for light neutralinos [70]. Depending on the neutralino mass the tree-level decay modes might be kinematically inaccessible while the radiative mode has, essentially, no threshold. Even in scenarios where both modes are possible, the radiative decay becomes particularly important for very light neutralinos as the mass dependence makes evident: $(m_{\tilde{\chi}_1^0}^3 m_f^2)/m_{\tilde{f}}^4$, *cf.* Eq. (2.12), against $m_{\tilde{\chi}_1^0}^5/m_{\tilde{f}}^4$ for the tree-level three-body decay into leptons, *cf.* Eq. (2.11).

3 Proton Decay Experiments

In this section, we present the proposed proton decay experiments that we focus on in this study: DUNE, JUNO, and Hyper-K. We summarize the important technical features for each detector in Table 1.

3.1 Detectors

DUNE, or the Deep Underground Neutrino Experiment [31–34], currently under construction, consists of a far detector (FD), situated 1.5 km underground at the Sanford Underground Research Facility (SURF), about 1300 km west of the Fermi National Accelerator Laboratory (FNAL). The FD is divided into four cuboidal detector volumes. Each has the dimensions 58.2 m × 14 m × 12 m and consists of modular Liquid Argon Time Projection Chambers (LArTPCs) with a fiducial mass of 10 kt. Charged particles ionize the medium and also produce scintillation light as they drift along the chamber. At the planned start of the beam run at FNAL, two FDs will be deployed, in two separate cryostat chambers. The first detector module is scheduled to be operational by 2026. In this work, we consider four chambers with a combined fiducial volume of 40 kt to derive our results, and assume that proton decays in one chamber are searched for in the same chamber, *i.e.* we do not consider the possibility that decays from one chamber are detected in another². Prototype studies estimate the detection efficiency at 30% for $p \rightarrow K^+ + \bar{\nu}$ [34]. The LArTPC technology

²The information on the spacing between the detectors and their arrangement is not clearly presented in the TDRs. Thus a combined analysis is currently not possible.

	Super-K	Hyper-K	JUNO	DUNE
Geometry	Cylindrical 42 m height \times 39 m diameter	Cylindrical 60 m height \times 74 m diameter	Spherical 35.4 m diameter	Cuboidal (4 modules) 58.2 m \times 14 m \times 12 m
Detector Material	Water	Water	LABs	Liquid Argon
Working Principle	Cherenkov	Cherenkov	Scintillation	Scintillation
Fiducial Mass	22.5 kt	187 kt	20 kt	40 kt
No. of Protons	$\sim 7.5 \times 10^{33}$	$\sim 6.3 \times 10^{34}$	$\sim 6.9 \times 10^{33}$	$\sim 1.1 \times 10^{34}$
$\epsilon_{inv.}$	$\mathcal{O}(10)\%$	$\mathcal{O}(10)\%$	37%	30%

Table 1: Summary of technical details for the upcoming detectors: **Hyper-K** [37], **JUNO** [35], and **DUNE** [31]. We include the characteristics of **Super-K** [81] for comparison. $\epsilon_{inv.}$ is the approximate detection efficiency of the charged kaon.

can, in principle, reduce the background below single-event level for key nucleon decay channels [31].

The Jiangmen Underground Neutrino Observatory, or **JUNO** [35, 36], is a proposed spherical liquid scintillator detector of inner diameter 35.4 m with 20 kt fiducial mass, situated 700 m underground at Kaiping in Southern China. It is expected to start operations in 2024. The current choice for the liquid scintillator material is linear alkylbenzene. The detector is submerged in a water pool to protect it from radioactivity from the surrounding rock and air. The expected background for $p \rightarrow K^+ + \bar{\nu}$ is 0.5 events per 10 years, and the expected detection efficiency reaches about 36.9% [92].

The Hyper-Kamiokande observatory, or **Hyper-K** [37], is the successor to the Super-Kamiokande (**Super-K**) experiment [81], and is a proposed large-scale underground water Cherenkov neutrino detector in Japan. Its proposed start of operations is around the year 2025. It consists of a cylindrical vertical tank with a diameter of 74 m and height of 60 m. The fiducial volume contains highly transparent purified water with a fiducial mass of about 187 kt. While most of the background is scattered by the surrounding water across the fiducial volume, or rejected through veto-detectors, neutron and kaon backgrounds from cosmic rays persist. Detection of the process $p \rightarrow K^+ + \bar{\nu}$ is achieved through the reconstruction of the pionic or muonic decay modes of the kaon. The former, owing to lower background, leads to stricter bounds. Its efficiency is expected to be about $10.8 \pm 1.1\%$. The corresponding expected background is 0.7 ± 0.2 red events per Mt per year.

3.2 Prospects for the Detection of the Neutralino Final State

Hyper-K offers a significantly higher fiducial volume, compared to the other detectors, but it is limited by its detection principle: **Hyper-K** (and **Super-K**) cannot measure the momentum for particles below the Cherenkov threshold of water, which for kaons, is about

750 MeV [80].³ This is a serious disadvantage for distinguishing between proton decay modes through a measurement of the momentum of the outgoing kaon, since the kaons from $p \rightarrow K^+ + \bar{\nu}$ are produced with a momentum of about 340, and the value is even lower in the case of a massive neutralino in the decay $p \rightarrow K^+ + \tilde{\chi}_1^0$, *cf.* Fig. 3. Thus, **Hyper-K** cannot distinguish the case of a kaon produced in association with a detector-stable (or invisibly decaying) massive neutralino from that of a decay involving a neutrino. Despite their smaller dimensions, **DUNE** and **JUNO** are very competitive in this respect: being scintillation detectors, they can measure the kinetic energy of the kaon down to a threshold of 50 MeV.

Turning to the detection strategy based on measuring the neutralino decay, we assume zero background and a neutralino detection efficiency, $\epsilon_{\text{vis.}}$, of 100% in our simulations. The characteristic signature includes visible objects from the kaon decay, as well as from the neutralino decay, with a likely displaced vertex structure. Timing-coincidence effects should provide us with various methods of implementing high-efficiency cuts leading to a clean signal-to-background ratio. However, the subsequent decay products of the neutralino, e.g. the muons and pions, might be invisible to the **Super-K** and **Hyper-K** detectors, again due to the threshold for Cherenkov radiation.⁴ The momenta of the muons and pions are fully determined by the mass and momentum of the parent neutralino. Depending on this momentum distribution, only a small fraction should induce Cherenkov radiation. Furthermore, due to the energy loss of the muons or pions, these should come to a stop inside the detector volume (in about 2 m) and produce characteristic subsequent decay products.

The muon, as well as the pion, can both be identified by a Michel electron. Thus, the event can be distinguished from competing processes by the identification of its final states. The preceding proton decay can be used as a trigger to reject background events. On the other hand, **DUNE** and **JUNO** can directly identify secondary particles in their tracking chambers. A precise estimate of their performance, taking into account the exact shape of the fiducial volume, would however require detailed simulations for each detector.

3.3 Proton Decay in Nuclei

In our discussion so far, we have considered free protons. Yet most of the protons in the detector materials are in bound states. **Super-K** and **Hyper-K** use water (H_2O) with most of the protons in the oxygen nucleus, **DUNE** uses liquid argon, and **JUNO** employs linear alkylbenzene ($\text{C}_6\text{H}_5\text{C}_n\text{H}_{2n+1}$) as proton sources. We now briefly discuss the impact of this distinction for our analysis.

Effects such as Fermi momentum, correlations between nucleons, and nuclear binding energy can alter the decaying proton's momentum, and thus the kaon momentum given in Eq. (2.10), in the lab frame. These effects can be analyzed through various approaches – for instance, by modeling the nucleus as a local Fermi gas [93], or through the so-called

³It can detect the kaon through its decay products since these are produced above the Cherenkov threshold.

⁴The Cherenkov threshold for muons is 160 MeV for the total energy, or 115 MeV for the kinetic energy. The threshold for charged pions is 210 MeV in the total energy and 160 MeV for the kinetic.

approximated spectral function approach [94, 95]. In addition, the produced kaon can re-scatter on the surrounding nucleons, further affecting its momentum, as it exits the nucleus. This can be modeled as a Bertini cascade [96–98], implemented in `GEANT4` [99, 100].

Due to the above effects, the kaon momentum is no longer fixed at the value of Eq. (2.10), but smeared out instead. A significant fraction of kaons lose energy, although some may also gain energy due to collisions with high-momentum nucleons. A detailed discussion for **Super-K** considering the ^{16}O nucleus can be found in Ref. [80]. A simulation for the case of argon can be found in Ref. [93]. A study for liquid scintillators can be found in Ref. [101], according to which we expect a comparable behavior with linear alkylbenzene.

For our study, the smearing effects are not expected to be of critical importance, since we do not attempt to simulate momentum measurements of the kaon, but focus instead on the search where the kaon is reconstructed through the observation of its decay products. This choice has a minor impact on the detection efficiency. For the momentum measurements, we will directly employ the sensitivity estimates claimed by the **DUNE** and **JUNO** collaborations. In the case of **Super-K** and **Hyper-K**, the kaon reconstruction relies on the kaon decaying at rest. Due to the effects discussed above, some kaons become energetic enough that they do not stop in the water before decaying. However, **Super-K** estimates this number to be only 11% [80].

In the case of **DUNE**, kaon tracks with a momentum higher than 180 MeV can be measured with a detection efficiency of 90% [34]. If the kaon momentum is below this threshold, the track cannot be reconstructed due to the short decay length of the kaon ($\beta\gamma\tau_K$). However, the reconstruction algorithms used in the experiment can still identify the kaon through its dominant decay chain, $K \rightarrow \mu \rightarrow e$, with an efficiency higher than 90%.⁵

For **JUNO** the search strategy relies on the observed time coincidence and well-defined energies of the kaon decay products [35]. Additionally, the liquid scintillator detects a prompt signal coming from the kaon. We assume that the efficiency for kaon reconstruction with this approach is constant for all momenta. A later study [92] indicates that the best reconstruction can be achieved by a time-correlated triple coincidence,

composed of the energy deposit of the kaon, a short-delayed deposit of its decay daughters and the energy deposit of the Michel electron from the muon decay. A detailed simulation of detector effects and proton momentum distribution for **DUNE** and **JUNO** would allow for an enhanced efficiency in the considered proton decay mode. However, this goes beyond the scope of this work.

Thus, we shall neglect any nuclear effects. However, we wish to emphasize that, in order to determine the mass of the neutralino from the kaon decay, a precise momentum measurement of the kaon is required. In that case, an accurate description of nuclear effects is crucial.

Before concluding this subsection, we briefly mention one more effect. A proton decaying inside a nucleus can leave the nucleus behind in an excited state. The latter de-excites

⁵A study performed by **DUNE** determined the detection efficiency for a kaon momentum in the range 150-450 MeV [34]. The efficiency can be up to $\sim 85\%$ for a kaon with a kinetic energy of 200 MeV. For kinetic energies below 50 MeV the efficiency is lower than for the reconstruction of the decay products, *i.e.* 30%. This efficiency is not used in our study but is claimed to be technically achievable.

promptly into the ground state by the emission of a gamma ray. One can estimate the energy of this photon and search for it as a coincidence signal. With this method, it is possible to reduce background events from cosmic ray muons and radioactivity of materials around the detector wall. Indeed, **Super-K** has searched for such gamma rays [80], and **Hyper-K** will be able to as well. **JUNO** can exploit the time-coincidence between the prompt signal from kaons hitting the liquid scintillator and a delayed signal from its decay products, to reduce background events. However, **DUNE** indicates that measuring time differences on the scale of the kaon lifetime is difficult [34].

3.4 Simulation Procedure

We now describe the simulation procedure that we use in order to estimate the sensitivities of the various experiments for detecting a proton decaying into a neutralino, possibly followed by the decay of the neutralino.

The total number of produced neutralinos (or kaons) in a given experimental setup may be written as,

$$N_{\tilde{\chi}_1^0}^{\text{prod}} = N_p \cdot \Gamma(p \rightarrow K^+ + \tilde{\chi}_1^0) \cdot t, \quad (3.1)$$

where $\Gamma(p \rightarrow K^+ + \tilde{\chi}_1^0)$ is calculated in Eq. (2.8), N_p is the total number of protons in the detector volume and t is the runtime of the experiment. If the neutralino is not explicitly looked for, the total number of observed events can then be estimated by simply multiplying the above expression by the efficiency of kaon detection, *cf.* discussion in the previous section.

In the case where the neutralino may decay visibly into a final state X , however, we also need to determine the number of such decays that can be reconstructed within the detector volume. We estimate them as,

$$N_{\tilde{\chi}_1^0 \rightarrow X}^{\text{obs.}} = N_{\tilde{\chi}_1^0}^{\text{prod}} \cdot \langle P[\tilde{\chi}_1^0 \text{ in d.r.}] \rangle \cdot \epsilon_{\text{vis.}}. \quad (3.2)$$

Here the function $\langle P[\tilde{\chi}_1^0 \text{ in d.r.}] \rangle$ represents the average probability of the neutralino to decay within the fiducial volume or the detectable region (d.r.) of the detector. This probability is dependent on the neutralino's lifetime, kinematics, point-of-origin within the detector, and the geometry of the detector itself. $\epsilon_{\text{vis.}}$, in the above, is the detection efficiency for the visible state X , which we shall ultimately set to 100% in this work, *cf.* Section 3.2.

In order to estimate $\langle P[\tilde{\chi}_1^0 \text{ in d.r.}] \rangle$ for each detector, we run a Monte Carlo simulation with $N_{\tilde{\chi}_1^0}^{\text{MC}}$ neutralinos of a given mass and with fixed RPV couplings.⁶ The neutralinos originate at random points within the detector, and travel in random directions. We discuss the geometry details for each detector below. Then, we estimate,

$$\langle P[\tilde{\chi}_1^0 \text{ in d.r.}] \rangle = \frac{1}{N_{\tilde{\chi}_1^0}^{\text{MC}}} \sum_{i=1}^{N_{\tilde{\chi}_1^0}^{\text{MC}}} P_i[\tilde{\chi}_1^0 \text{ in d.r.}], \quad (3.3)$$

where,

$$P_i[\tilde{\chi}_1^0 \text{ in d.r.}] = 1 - e^{-L_i/\lambda}, \quad (3.4)$$

⁶In practice, we set $N_{\tilde{\chi}_1^0}^{\text{MC}}$ to a value of about 10,000 to 50,000 events.

is the individual probability for the i^{th} simulated neutralino to decay inside the detector. L_i is the distance between the point where the neutralino originates and the detector boundary along its direction-of-travel. The mean decay length λ (independent of i) is given by,

$$\lambda = \gamma\beta/\Gamma_{\text{tot}}, \quad (3.5)$$

with Γ_{tot} the total decay width of the neutralino and,

$$\gamma = E/m_{\tilde{\chi}_1^0}, \quad \beta = \sqrt{\gamma^2 - 1}/\gamma. \quad (3.6)$$

In the above, $m_{\tilde{\chi}_1^0}$ and E are the neutralino mass and energy, respectively. Thus, L_i is the only geometry-dependent factor. We now describe how we calculate it for the considered detectors.

Hyper-K: Hyper-K is a vertical cylindrical-shaped detector with a radius of $R = 37$ m and height $H = 60$ m. Let the i^{th} neutralino be generated inside the Hyper-K volume at a point (r, φ, z) in a cylindrical coordinate system with origin at the center of the bottom surface ($z = 0$) of the detector. Let its three-velocity, \vec{v} , be at azimuthal angle φ_v with components v_z and $v_{\perp} = \sqrt{\vec{v}^2 - v_z^2}$ along the z -axis and in the polar plane, respectively. Then, we have,

$$L_i = |\vec{v}| \times \min(t_1, t_2), \quad (3.7)$$

where,

$$t_1 \equiv \begin{cases} \frac{(H - z)}{v_z}, & \text{if } v_z > 0, \\ -\frac{z}{v_z}, & \text{if } v_z < 0, \end{cases} \quad (3.8)$$

and $t_1 > t_2$ if $v_z = 0$. Here, t_2 is given by,

$$t_2 = \frac{-r\cos(\varphi - \varphi_v) + \sqrt{R^2 - r^2\sin^2(\varphi - \varphi_v)}}{|v_{\perp}|}. \quad (3.9)$$

Super-K can be modeled analogously.

DUNE: DUNE has four cuboid-shaped FDs with dimensions $L = 58.2$ m, $W = 14.0$ m, and $H = 12.0$ m. In a rectangular coordinate system with the origin at the bottom corner of the detector, for the i^{th} neutralino generated at (x, y, z) traveling towards the direction denoted by the three-vector $\vec{v} = (v_x, v_y, v_z)$, we define,

$$t_x \equiv \begin{cases} \frac{(L - x)}{v_x}, & \text{if } v_x > 0, \\ -\frac{x}{v_x}, & \text{if } v_x < 0, \end{cases} \quad (3.10)$$

and $t_x > t_y, t_z$ if $v_x = 0$, and analogous expressions for t_y and t_z , depending on W, H , respectively. L_i is then given by,

$$L_i = |\vec{v}| \times \min(t_x, t_y, t_z). \quad (3.11)$$

JUNO: JUNO has a spherical geometry with a radius of $R_{\max} = 17.7$ m. For a neutralino produced at a random point $\vec{r} = (r_i, \theta_i, \varphi_i)$ inside the detectable region and with velocity \vec{v} , flying in the direction given by the angles (θ_j, φ_j) , one can calculate the angle θ between the two vectors: $\cos \theta = \frac{\vec{r} \cdot \vec{v}}{|\vec{r}| |\vec{v}|}$. A coordinate transformation is performed in order to eliminate the dependence of θ on φ_i, φ_j , such that $\theta = \theta_i - \theta_j \in [0, 2\pi]$. The final distance is calculated to be:

$$L_i = -r_i \cos(\theta) + \sqrt{R_{\max}^2 - r_i^2 \sin^2(\theta)}. \quad (3.12)$$

As an illustration, we depict $\langle P[\tilde{\chi}_1^0 \text{ in d.r.}] \rangle$ in Fig. 4 as a function of the neutralino mass but for fixed decay length, $c\tau$, for the four detectors. The neutralino momentum $p_{\tilde{\chi}_1^0}$ at production depends on the neutralino mass $m_{\tilde{\chi}_1^0}$ as in Eq. (2.10). Thus for increasing $m_{\tilde{\chi}_1^0}$, $|\vec{v}_{\tilde{\chi}_1^0}|$ decreases, and the neutralino is more likely to decay in the detector for a fixed lifetime.

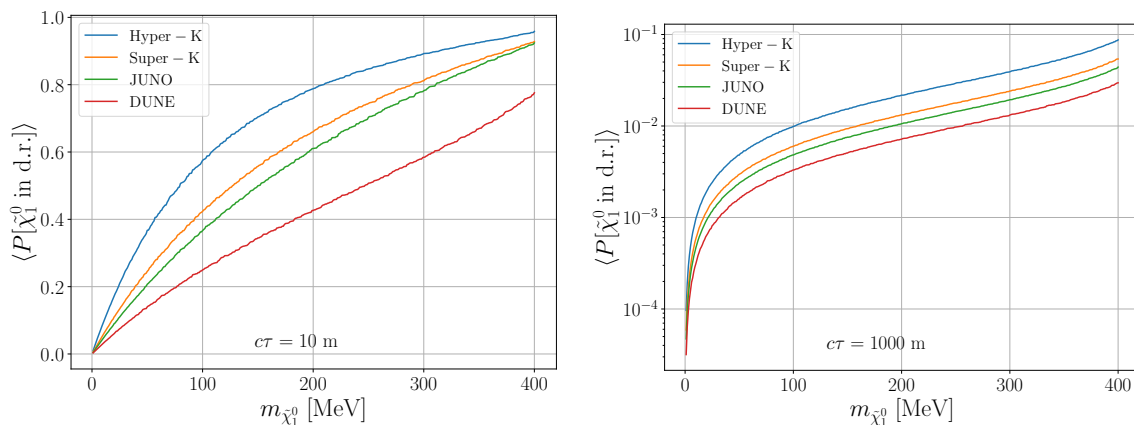


Figure 4: Average neutralino decay probabilities as a function of the neutralino mass for fixed neutralino decay length: $c\tau = 10$ m (left) and $c\tau = 1000$ m (right). These plots have been generated with a sample size $N_{\tilde{\chi}_1^0}^{\text{MC}} = 10,000$.

4 Numerical Analysis

We now present benchmark scenarios, which, we believe, capture the bulk of the phenomenology accessible at DUNE, JUNO and Hyper-K for a proton decaying to a lighter neutralino. In all the considered cases, the proton disintegration is controlled by the parameter λ''_{121} , as in Eq. (2.8). Thus, we only consider cases for which $m_{\tilde{\chi}_1^0} \lesssim 445$ MeV, *cf.* Eq. (1.1). The produced neutralino either escapes the detector as missing energy or decays into visible modes via an RPV operator λ_{ijk}^D . The benchmarks we study are presented in Section 4.1 and summarized in Table 2. We present the corresponding numerical studies in Section 4.2. For each scenario, we assume that the listed couplings are the only non-negligible RPV couplings; the relevant current bounds are also shown in the table.

Scenario	$m_{\tilde{\chi}_1^0}$	Proton Decay	$\tilde{\chi}_1^0$ Decay (λ_{ijk}^D)	Product Bound	Min. $c\tau_{\tilde{\chi}_1^0}$
B1	0 – 400 MeV	$\lambda''_{121} < 5 \times 10^{-7} \left(\frac{m_{\tilde{q}}}{\Lambda\text{TeV}}\right)^{5/2}$	–	–	∞
B2	0 – 400 MeV	$\lambda''_{121} < 5 \times 10^{-7} \left(\frac{m_{\tilde{q}}}{\Lambda\text{TeV}}\right)^{5/2}$	$\lambda'_{333} < 1.04$	$\lambda'_{333}\lambda''_{121} < 10^{-9}$	~ 1600 m
B3	0 – 400 MeV	$\lambda''_{121} < 5 \times 10^{-7} \left(\frac{m_{\tilde{q}}}{\Lambda\text{TeV}}\right)^{5/2}$	$\lambda_{233} < 0.7 \left(\frac{m_{\tilde{\tau}_R}}{1\text{TeV}}\right)$	$\lambda_{233}\lambda''_{121} < 10^{-21}$	~ 180 m
B4	150 – 400 MeV	$\lambda''_{121} < 5 \times 10^{-7} \left(\frac{m_{\tilde{q}}}{\Lambda\text{TeV}}\right)^{5/2}$	$\lambda'_{211} < 0.59 \left(\frac{m_{\tilde{d}_R}}{1\text{TeV}}\right)$	$\lambda'_{211}\lambda''_{121} < 6 \times 10^{-25}$	~ 11 m
B5	150 – 400 MeV	$\lambda''_{121} < 5 \times 10^{-7} \left(\frac{m_{\tilde{q}}}{\Lambda\text{TeV}}\right)^{5/2}$	$\lambda'_{311} < 1.12$	$\lambda'_{311}\lambda''_{121} < 4 \times 10^{-24}$	~ 8 m

Table 2: Details of the benchmark scenarios. The bounds on λ_{ijk}^D are taken from Refs. [102, 103] while the one on λ''_{121} is from Ref. [104]. Product bounds are obtained from Ref. [41] for SUSY masses of 1 TeV, except in the case of $\lambda'_{311}\lambda''_{121}$, where it is the bound on $p \rightarrow K^+ + \bar{\nu}$ from [80] reinterpreted for **B5**. The mass ranges conform (up to some rounding) to the discussion in the text. An additional limit originates from Super-K: $|\lambda''_{121}| < 3.9 \times 10^{-31} \left(\frac{m_{\tilde{q}}}{\text{GeV}}\right)^2$. “Min. $c\tau_{\tilde{\chi}_1^0}$ ” refers to the minimal decay length, *i.e.* the decay length at the maximal allowed RPV coupling and neutralino mass within the scenario.

4.1 Benchmark Scenarios

In the first benchmark scenario, **B1**, we assume that the neutralino cannot be observed at DUNE, JUNO or Hyper-K, either due to a long lifetime or to invisible decay products. (We set L -violating couplings to 0 in practice.)

In the second benchmark, **B2**, neutralino decays are controlled by the trilinear coupling λ'_{333} . In this case tree-level decay modes [$\tilde{\chi}_1^0 \rightarrow (\tau^- t\bar{b}, \nu_\tau b\bar{b})$] are kinematically prohibited, under the assumption of negligible generation mixing [87, 88]. The radiative channel, mediated by (s)bottom loops, then appears as the dominant one. Existing limits on λ'_{333} imply an already sizable decay length (see the last column of Table 2), as compared to the dimensions of the experiments (listed in Table 1). We briefly comment on alternative choices of dominant λ'_{ijj} couplings controlling the radiative decay mode of the neutralino. Due to the scaling with the fermion mass squared [see Eq. (2.12)], we can dismiss the cases $j = 1, 2$ as resulting in very long lifetimes. The choice of a dominant λ'_{133} offers little competition as well, due to severe experimental bounds [102, 103]: $|\lambda'_{133}| < 1.4 \times 10^{-3} \sqrt{\left(\frac{m_{\tilde{q}}}{100\text{GeV}}\right)}$. λ'_{233} should perform comparably to λ'_{333} retained here.

Benchmark **B3** also involves radiative neutralino decays, now controlled by the trilinear coupling λ_{233} leading to a tau/stau loop. In this case, significantly shorter decay lengths are accessible (see Table 2), as compared to **B2**. Other choices of λ_{ijj} would yet lead to very long decay lengths again, if $j = 1, 2$, while λ_{133} is severely constrained experimentally.

The two last scenarios involve tree-level decay modes of the neutralino. Here, we dismiss leptonic decays, since the widths associated with Eq. (2.11) lead to very long-lived neutralinos, escaping the detectors in the considered mass regime. Similarly, a very strict experimental limit on λ'_{111} [103] leaves only λ'_{211} and λ'_{311} in a position to generate semi-leptonic disintegrations of the neutralino that are observable at DUNE, JUNO, or Hyper-K. For **B4**, a non-vanishing λ'_{211} potentially opens the semi-leptonic modes: $\tilde{\chi}_1^0 \rightarrow \pi^\pm + \mu^\mp$, $\tilde{\chi}_1^0 \rightarrow \pi^0 + \nu_\mu$, $\pi^0 + \bar{\nu}_\mu$, with kinematical limits on the neutralino mass reading $m_{\pi^\pm} + m_{\mu^\mp} \leq$

$m_{\tilde{\chi}_1^0} < m_p - m_{K^+}$ and $m_{\pi^0} \leq m_{\tilde{\chi}_1^0} < m_p - m_{K^+}$, respectively. In benchmark **B5**, $\lambda'_{311} \neq 0$ triggers the decay channel $\tilde{\chi}_1^0 \rightarrow \pi^0 + \nu_\tau$ provided $m_{\pi^0} \leq m_{\tilde{\chi}_1^0} < m_p - m_{K^+}$. The $SU(2)_L$ -related charged channel is kinematically closed. In both cases, the radiative decay mode mediated by a down/sdown loop, although open, results in negligible widths due to the Yukawa suppression.

4.2 Results

We may now discuss the experimental prospects for each of the proposed benchmark scenarios. For commodity, we dismiss the comparatively broad theoretical uncertainties exemplified by Fig. 2, *i.e.* work with an absolute prediction of the decay rates, as obtained with the hadronic input of Ref. [84], and strictly focus on a comparative analysis of the various experiments in view of identifying a signal of the studied kind. This means that the (prospective) bounds on the parameter space of the RPV-MSSM shown below should not be understood as absolute, but still require a proper account of the theoretical uncertainties before any attempt at correlating them with input from other observables.

In the case of **B1**, with a stable, *i.e.* invisible, neutralino at the detector scale, we present in Fig. 5 the projected parameter space coverage achieved by DUNE [34], JUNO [92] and Hyper-K [37] at 90% confidence level sensitivity, after a ten-year run time. Here, we recast the projections quoted for the $p \rightarrow K^+ + \bar{\nu}$ mode in the technical reports, under the assumption that these remain valid with the modified kaon kinematics. For Hyper-K, where the kaon momentum is not measurable, the cases of a massive or massless neutralino are indeed indistinguishable⁷ and our working hypothesis amounts to modeling the signal efficiencies and experimental backgrounds as roughly constant in the considered kinematical window, as discussed in Section 3. The current Super-K bound [80] can be exploited in the same fashion, and is included in the plot. For DUNE and JUNO, however, the searches implement specific cuts on the kaon momentum in order to reduce the background due to atmospheric neutrinos. This implies that the actual bounds in the massive case would be weaker than the naive one, due to eroded signal efficiency. Nevertheless, it might be possible to optimize the momentum cuts in searches dedicated to the massive neutralino case and counteract this diminished sensitivity. A more precise detector simulation goes beyond the scope of the current paper.

Fig. 5 shows the parameter space explored by the various experiments in the plane spanned by the neutralino mass $m_{\tilde{\chi}_1^0}$ and $\lambda''_{121}/m_{\tilde{f}}^2$. The proton decay rate is kinematically suppressed as the neutralino mass approaches the threshold, $m_{\tilde{\chi}_1^0} < 445$ MeV; this weakens the reach in $\lambda''_{121}/m_{\tilde{f}}^2$ as compared to the massless case. JUNO, DUNE and Hyper-K are all expected to improve on the coverage achieved at Super-K, probing values of $\lambda''_{121}/m_{\tilde{f}}^2$ as much as 1.3, 1.5 and 2.5 smaller, respectively. Thus, despite Hyper-K's advantage in terms of fiducial mass, JUNO and DUNE remain competitive thanks to their superior efficiencies and high background-rejection rates. In addition, we stress that momentum measurements of the produced kaon, needed to correlate the rate with the neutralino mass, will only be

⁷Most kaons ($\sim 80\%$) decay at rest, and in this case the muons carry no information relative to the momentum of their parent kaons.

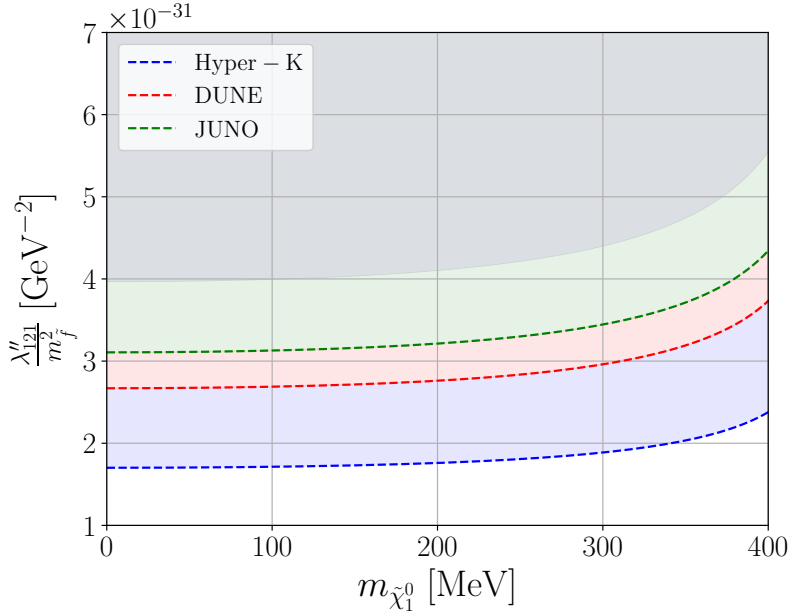


Figure 5: Sensitivity reach for the single coupling scenario of benchmark **B1**. The reinterpreted bound from **Super-K** is shown in gray. The bound from Table 2 lies above the scale of the plot. The results for **Hyper-K**, **DUNE**, and **JUNO** are for a run-time of 10 years.

possible at these two experiments. While the current level of information presented in technical reports and the difficulty of modeling the macroscopic effects leading to momentum smearing make it impossible for us to realistically simulate this search, one should keep in mind that this observable would be simultaneously available with the kaon detection search, and might allow **DUNE** or **JUNO** to distinguish the scenario with a neutralino from its counterpart with a neutrino, even if both these final states result in missing energy at colliders.

We now turn to the scenarios with a visible neutralino decay. In this case, the relevant parameter space is (at least) three-dimensional, consisting of $m_{\tilde{\chi}_1^0}$, λ''_{121}/m_f^2 (controlling the proton decay, and thus the production rate of the neutralinos), and $\lambda_{ijk}^{(l)}/m_f^2$ (controlling the neutralino decay together with the neutralino mass). For commodity, we focus on two projections in this parameter space:

- First, we examine the plane λ''_{121}/m_f^2 vs. $\lambda_{ijk}^{(l)}/m_f^2$ at $m_{\tilde{\chi}_1^0} \stackrel{!}{=} 400$ MeV.
- Then, we consider the plane λ_{ijk}^D/m_f^2 vs. $m_{\tilde{\chi}_1^0}$, with λ''_{121}/m_f^2 set to its value saturating the reinterpreted bound from **Super-K**. The corresponding values of λ''_{121}/m_f^2 as a function of the neutralino mass would correspond to the edge of the gray area in Fig. 5 in the case of a purely invisible decay of the neutralino, but are actually shifted when a shorter lifetime makes the invisible search less relevant.

In both cases, we also indicate the neutralino decay lengths, as this observable is directly correlated with the considered neutralino decay coupling. Again, we assume an accumulated

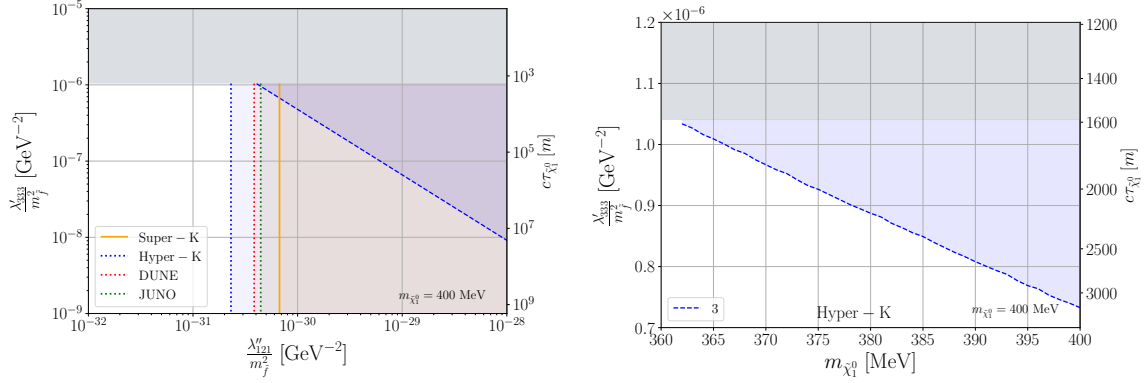


Figure 6: Sensitivity reach/Super-K limit for benchmark **B2**. The existing single-bound on λ'_{333} from Table 2 is shown in gray (with $m_{\tilde{f}} = 1$ TeV), while the product-bound lies outside the scale of the plot. *Left:* The limits in the coupling-vs.-coupling plane with $m_{\tilde{\chi}_1^0} = 400$ MeV. The contours correspond to the visible mode (blue dashed, downward sloping line) and invisible mode (vertical lines); see discussion in the text. *Right:* The limits in the coupling-vs.-mass plane for the visible mode with $\lambda''_{121}/m_{\tilde{f}}^2$ fixed at the threshold of the Super-K bound of Fig. 5.

ten years of observed data at DUNE, JUNO and Hyper-K. As we neglect any sort of background, the reach corresponding to 95% confidence level exclusion is determined by the 3-event isocurves, which we display in our plots.⁸ Existing constraints of Table 2 are also depicted in gray (single-bounds) or cyan (product-bounds), where relevant.

We then consider the benchmark **B2** with a still long-lived neutralino decaying radiatively via bottom / sbottom loops. The corresponding results are shown in Fig. 6. Experiments are sensitive to this scenario from two directions. First, most of the neutralinos decay outside the detectors, due to their long lifetime, hence appear as missing energy, similarly to the scenario of Fig. 5. In fact, consulting the right plot of Fig. 4, we observe that this happens for over 90% of the neutralinos, on average, even for the shortest available lifetimes and a mass as large as $m_{\tilde{\chi}_1^0} = 400$ MeV. The corresponding bound hardly depends on $\lambda'_{333}/m_{\tilde{f}}^2$ (as long as one is deep in this long-lived regime) and produces vertical boundary lines in the plane spanned by $\lambda''_{121}/m_{\tilde{f}}^2$ and $\lambda'_{333}/m_{\tilde{f}}^2$, as displayed on the left-hand side of Fig. 6. Larger values of $\lambda''_{121}/m_{\tilde{f}}^2$ can be probed (or, in case of Super-K, are already excluded) by the invisible neutralino search. A subsidiary region is probed by the visible search, where only the 3-event line associated with Hyper-K appears on the plot (the corresponding boundaries for DUNE and JUNO would be far to the right). We should stress, here, that our estimates for the efficiencies achieved in the visible search are very optimistic and that the reach of this observable may be significantly more reduced than what is presented in Fig. 5. The number of visible decays scales like $|\lambda'_{333}\lambda''_{121}/m_{\tilde{f}}^4|^2$ in the limit of long neutralino lifetimes, resulting in a sloping coverage limit. The large volume of Hyper-K is a clear advantage for detection sensitivity.

⁸Where relevant, we also depict 30- and 90-event isocurves.

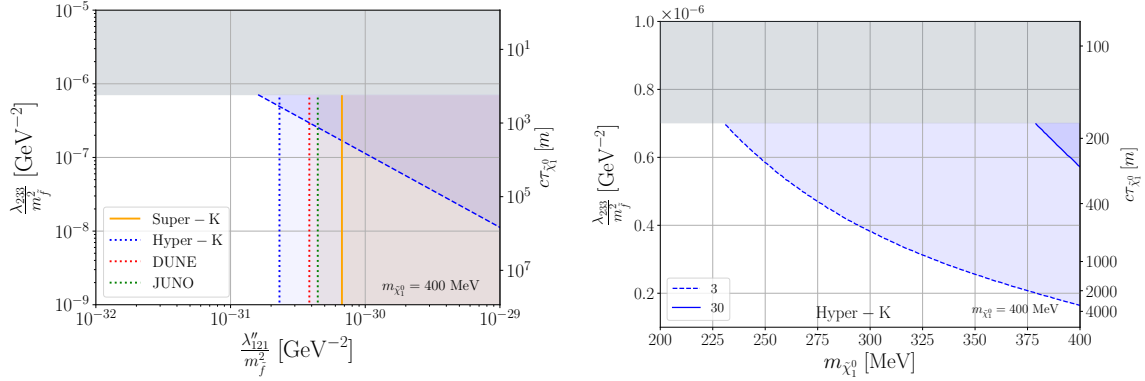


Figure 7: Sensitivity reach/**Super-K** limit for benchmark **B3**. The existing single-bounds from Table 2 are shown in gray while the product-bound is shown in blue (all with $m_{\tilde{f}} = 1$ TeV). *Top Left:* As in left plot of Fig. 6 but for benchmark **B3**. *Top Right:* Zoomed-out version of the top-left plot. *Bottom:* As in right plot of Fig. 5 but for benchmark **B3**. The dashed and solid lines correspond to 3- and 30-event isocurves, respectively.

In the right plot of the figure, we show the sensitivity reach of the visible mode in the $\lambda'_{333}/m_{\tilde{f}}^2$ vs. $m_{\tilde{\chi}_1^0}$ plane, where $\lambda'_{121}/m_{\tilde{f}}^2$ is always set at the exclusion limit of **Super-K**.⁹ The sensitivity improves as the neutralino mass increases due to (a) the lifetime becoming shorter, *cf.* Eq. (2.12), and (b) the neutralinos having lower momentum: the decay length of the neutralino ($\beta\gamma c\tau$) $_{\tilde{\chi}_1^0}$ is indeed shorter, resulting in an increased average decay sensitivity ($\langle P[\tilde{\chi}_1^0 \text{ in d.r.}] \rangle$), as shown in Fig. 4.

The physics situation of benchmark **B3** is largely comparable to that of the former benchmark, with a radiatively decaying neutralino. Consequently, the parameter space coverage in proton decay experiments follows the same trends, as can be observed in Fig. 7. Shorter lifetimes are accessible nonetheless, resulting in an increased relevance of the visible search channel, although only **Hyper-K** has viable detection prospects in this mode. The left-hand plot of Fig. 7 distinctly exhibits a region in the higher range of $\lambda'_{233}/m_{\tilde{f}}^2$ where both types of detection are competitive, as well as a tiny region only accessible to the visible search. Once again, we point at the generous efficiencies assumed for the visible search here: this region accessible only to the visible search would likely shrink with more realistic estimates.

In the case of benchmarks **B4** and **B5**, the tree-level decay modes of the neutralino may result in comparatively short lifetimes when the RPV couplings are set to their maximal values compatible with existing bounds. As a consequence, the visible search strategy is expected to perform more competitively than for the previous scenarios. Our results are shown in Fig. 8 and Fig. 9. There, a portion of the parameter space left open by **Super-K** is accessible to visible searches at **DUNE** or **JUNO**, although **Hyper-K** remains the experiment most sensitive to this mode (as well as to the invisible search). Conversely, the invisible search channel becomes less competitive in the higher range of $\lambda'_{211}/m_{\tilde{f}}^2$ due to fewer neu-

⁹All the corresponding points are thus simultaneously, and independently, probed by the invisible search at **Hyper-K**, **DUNE**, and **JUNO**.

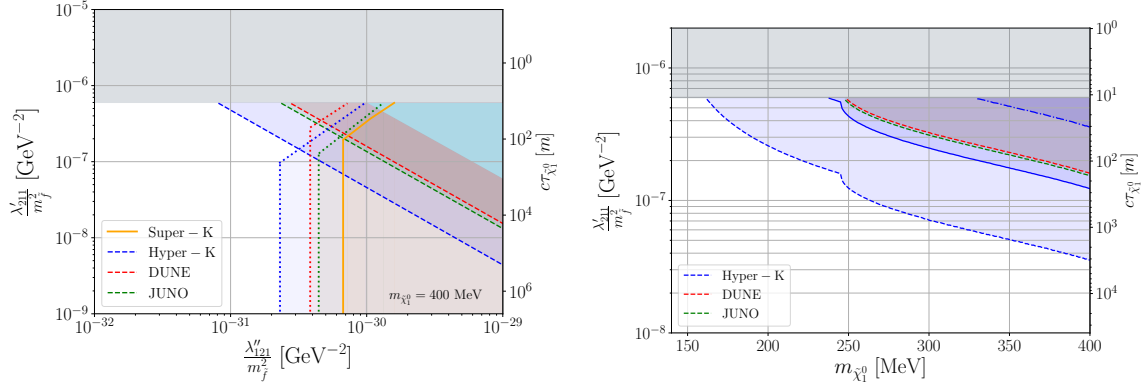


Figure 8: Sensitivity reach/Super-K limit for benchmark **B4**. The existing single-bound on λ'_{211} from Table 2 is shown in gray, the product-bound is in light blue (both with $m_{\tilde{f}} = 1$ TeV), while the bound on λ''_{121} lies outside the scale of the plot. *Left:* As in left plot of Fig. 6 but for benchmark **B4**. *Right:* As in right plot of Fig. 5 but for benchmark **B4**. The dashed, solid, and dot-dashed lines correspond to 3-, 30- and 90-event isocurves, respectively. An interesting thing to note is the kink in sensitivity in the right figure around $m_{\tilde{\chi}_1^0} \sim 240$ MeV, which is due to the modes $\tilde{\chi}_1^0 \rightarrow \pi^\pm + \mu^\mp$ being kinematically allowed, thus increasing the total decay width.

tralinolinos escaping the detectors: this effect is observable as a kink in the boundaries, which transit from the $\lambda'_{i11}/m_{\tilde{f}}^2$ -blind regime at $\lambda'_{211}/m_{\tilde{f}}^2 \lesssim 10^{-7}$ to a power-law regime (appearing as a line in logarithmic scales). Interestingly, DUNE proves slightly more performant than Hyper-K in the upper range of $\lambda'_{i11}/m_{\tilde{f}}^2$ for the invisible search.

To summarize this discussion, we observed that the invisible search strategy remains highly relevant for long-lived neutralinos produced in proton decays, with an evident advantage in regions of the parameter space where neutralino decays are suppressed, *i.e.* in the lower range of the L-violating trilinear couplings or in the regime dominated by radiative decays. There, DUNE, JUNO and Hyper-K would typically improve on Super-K by a factor 2. We nonetheless stress that this performance depends on the validity of the reinterpretation of the searched massless neutrino in terms of a massive neutralino. Here, the measurement of the kaon momentum, possible at DUNE or JUNO in principle, could help discriminate between the two cases and hint at a neutralino-like scenario. On the other hand, the visible search channel allows for a complementary and largely independent coverage of parameter space when L-violating \tilde{f} effects are sufficiently large to enhance the number of neutralinos decaying in the detectors. Such a signal would be a clear indication for a proton decay mode beyond the straightforward (and possibly also supersymmetric) $K^+ + \bar{\nu}$ channel. In a narrow region of the RPV-MSSM parameter space, both visible and invisible strategies could be simultaneously successful and result in observations at one (not necessarily the same) of the three planned experiments. A statistical combination of the two signals would then be possible, leading to an expectedly even higher sensitivity. Finally, we wish to stress the impact of one of our working assumptions: with more than one non-zero L-violating couplings, multiple decay channels would open for the neutralino, leading to an increased

relevance of the visible over the invisible search strategy.

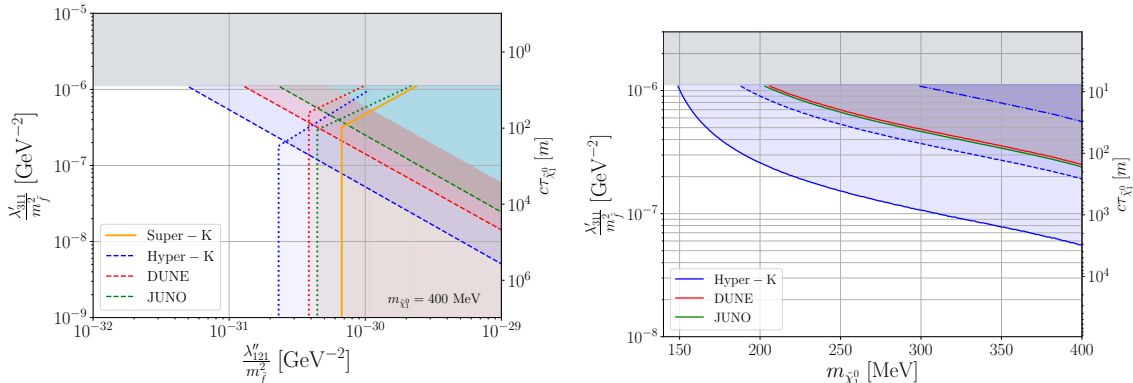


Figure 9: Sensitivity reach/Super-K limit for benchmark **B5**. The existing single-bound on λ'_{311} from Table 2 is shown in gray, the product-bound is in light blue (both with $m_{\tilde{f}} = 1$ TeV), while the bound on λ''_{121} lies outside the scale of the plot. *Left:* As in left plot of Fig. 6 but for benchmark **B5**. *Right:* As in right plot of Fig. 5 but for benchmark **B5**. The dashed, solid, and dot-dashed lines correspond to 3-, 30- and 90-event isocurves, respectively.

5 Conclusions

The search for proton decay is tightly related to the fundamental and experimentally well-established question of matter-antimatter asymmetry. Experimental and phenomenological activity in this respect thus appears strongly motivated. In this work, we tried to emphasize a less standard but very realistic decay mode of the proton, $p \rightarrow K^+ + \tilde{\chi}_1^0$. Here $\tilde{\chi}_1^0$ denotes a light and long-lived exotic neutral particle, e.g. a bino-like neutralino in the RPV-MSSM, which can possibly decay within the detector. We demonstrate the strong potential of the upcoming DUNE, JUNO and Hyper-K experiments to investigate such a scenario. This analysis was performed under the assumption that the experimental searches considering a massless neutrino can be reinterpreted in terms of a massive exotic particle, or that experimental cuts can be adjusted in order to address this situation. Several signatures can be looked for, depending on the lifetime of the neutralino and its decay channels. Measurement of the kaon momentum (at DUNE or JUNO) or observation of a displaced vertex from the neutralino decay would provide means to distinguish such a scenario from the more traditionally considered $p \rightarrow K^+ + \bar{\nu}$. We have illustrated these features with the help of a collection of benchmarks. A significant coverage of the parameter space can be achieved by DUNE, JUNO and, most especially, Hyper-K, clearly improving on the current limits obtained at Super-K. More detailed collider simulations would be necessary to precisely delimit the reach of these experiments. In any case, we stress the necessity to keep the scope of the experiments as broad as possible and allow the reinterpretation of results in non-standard scenarios.

Acknowledgments

We thank Artur Ankowski, Marcela Carena, Felix Kling, Ornella Palamara, Rob Timmermans, Simon Zeren Wang, and Tingjun Yang for useful discussions. HKD thanks the Nikhef theory group for its hospitality while part of this work was completed. This work was supported by the Deutsche Forschungsgemeinschaft (DFG, German Research Foundation) through the funds provided to the Sino-German Collaborative Research Center TRR110 “Symmetries and the Emergence of Structure in QCD” (DFG Project ID 196253076 - TRR 110).

A Heavy Neutral Lepton

Throughout our work we have focussed on decays to and of a supersymmetric neutralino in a model with broken R-parity. As explained in Section 2, the low-energy (proton-scale) EFT’s of Refs. [51, 86] provide a natural framework to study such processes. The imprint of the high-energy (in our case SUSY) model is then encoded within the Wilson coefficients, determined by the matching procedure and the Renormalization Group Equations. In this fashion, we were always able to present our results in terms of the parameters of the more fundamental model, namely the neutralino mass $m_{\tilde{\chi}_1^0}$, the RPV couplings λ''_{ijk} , λ'_{ijk} , λ_{ijk} , and the universal scalar fermion mass $m_{\tilde{f}}$. In the production of the neutralino via proton decay baryon-number is violated. In the decay of the neutralino lepton-number is violated. Here, we have associated no lepton- or baryon- number with the (Majorana) neutralino.

As outlined in the introduction a right-handed neutrino, N_R , potentially light, has the same SM gauge quantum numbers as the light (dominantly bino) neutralino. Associating the lepton number 1 with such a Majorana particle, N_R , thus appears as a largely formal distinction in the L-violating context and the expected phenomenology in proton disintegrations is formally unchanged. In particular, the proton-scale EFT’s of Refs. [51, 86] (with the neutralino replaced by N_R) remain fully operational intermediaries between high-energy scales and hadronic physics. Differences of the UV completion in the neutralino case (RPV-SUSY) and any potential UV completion for the HNL model will emerge at the level of the matching.

The phenomenology of the right-handed neutrino can be studied in the context of ν SMEFT [105–107], itself a low-energy EFT valid at the electroweak scale. Obvious contributions to the proton-decay operators are generated by the operators listed in Eq. (7) in Ref. [105]. We insist upon the fact that these contributions from ν SMEFT potentially involve low-energy operators beyond \hat{Q}'_1 , \hat{Q}_1 , \hat{Q}_2 of Eq. (2.4). Indeed, SUSY (through the holomorphicity condition of the superpotential) favors baryon-number violation involving right-handed [*i.e.* SU(2)-singlet] quarks, while such a prejudice need not apply in ν SMEFT.¹⁰

Similarly, the ν SMEFT operators listed in Eq. (6) in Ref. [105] and denoted \mathcal{O}_{LNLe} , \mathcal{O}_{LNQd} , and \mathcal{O}_{QNLd} straightforwardly contribute to the decays of the right-handed neutrino.

¹⁰Even in the RPV-MSSM, contributions restrict to the operators \hat{Q}'_1 , \hat{Q}_1 , \hat{Q}_2 only under simplifying assumptions regarding *e.g.* the mixing among SUSY particles.

Corresponding effects can be projected onto the low-energy operator list presented in detail in Ref. [86], in the context of a light neutralino.

References

- [1] G. Steigman, *Observational tests of antimatter cosmologies*, *Ann. Rev. Astron. Astrophys.* **14** (1976) 339–372.
- [2] L. Canetti, M. Drewes, and M. Shaposhnikov, *Matter and Antimatter in the Universe*, *New J. Phys.* **14** (2012) 095012, [[arXiv:1204.4186](#)].
- [3] A. D. Sakharov, *Violation of CP Invariance, C asymmetry, and baryon asymmetry of the universe*, *Pisma Zh. Eksp. Teor. Fiz.* **5** (1967) 32–35.
- [4] G. 't Hooft, *Computation of the Quantum Effects Due to a Four-Dimensional Pseudoparticle*, *Phys. Rev. D* **14** (1976) 3432–3450. [Erratum: *Phys.Rev.D* 18, 2199 (1978)].
- [5] N. S. Manton, *Topology in the Weinberg-Salam Theory*, *Phys. Rev. D* **28** (1983) 2019.
- [6] J. A. Harvey and M. S. Turner, *Cosmological baryon and lepton number in the presence of electroweak fermion number violation*, *Phys. Rev. D* **42** (1990) 3344–3349.
- [7] H. K. Dreiner and G. G. Ross, *Sphaleron erasure of primordial baryogenesis*, *Nucl. Phys. B* **410** (1993) 188–216, [[hep-ph/9207221](#)].
- [8] V. A. Kuzmin, V. A. Rubakov, and M. E. Shaposhnikov, *On the Anomalous Electroweak Baryon Number Nonconservation in the Early Universe*, *Phys. Lett. B* **155** (1985) 36.
- [9] M. E. Shaposhnikov, *Baryon Asymmetry of the Universe in Standard Electroweak Theory*, *Nucl. Phys. B* **287** (1987) 757–775.
- [10] M. B. Gavela, P. Hernandez, J. Orloff, and O. Pene, *Standard model CP violation and baryon asymmetry*, *Mod. Phys. Lett. A* **9** (1994) 795–810, [[hep-ph/9312215](#)].
- [11] M. B. Gavela, P. Hernandez, J. Orloff, O. Pene, and C. Quimbay, *Standard model CP violation and baryon asymmetry. Part 2: Finite temperature*, *Nucl. Phys. B* **430** (1994) 382–426, [[hep-ph/9406289](#)].
- [12] H. Georgi and S. L. Glashow, *Unity of All Elementary Particle Forces*, *Phys. Rev. Lett.* **32** (1974) 438–441.
- [13] J. Wess and B. Zumino, *Supergauge Transformations in Four-Dimensions*, *Nucl. Phys. B* **70** (1974) 39–50.
- [14] J. Wess and B. Zumino, *A Lagrangian Model Invariant Under Supergauge Transformations*, *Phys. Lett. B* **49** (1974) 52.
- [15] R. Haag, J. T. Lopuszanski, and M. Sohnius, *All Possible Generators of Supersymmetries of the s Matrix*, *Nucl. Phys. B* **88** (1975) 257.
- [16] H. P. Nilles, *Supersymmetry, Supergravity and Particle Physics*, *Phys. Rept.* **110** (1984) 1–162.
- [17] H. E. Haber and G. L. Kane, *The Search for Supersymmetry: Probing Physics Beyond the Standard Model*, *Phys. Rept.* **117** (1985) 75–263.
- [18] S. P. Martin, *A Supersymmetry primer*, *Adv. Ser. Direct. High Energy Phys.* **18** (1998) 1–98, [[hep-ph/9709356](#)].

- [19] H. K. Dreiner, H. E. Haber, and S. P. Martin, *From Spinors to Supersymmetry*. Cambridge University Press, Cambridge, UK, 7, 2023.
- [20] J. H. Schwarz, *Superstring Theory*, *Phys. Rept.* **89** (1982) 223–322.
- [21] M. B. Green, *Supersymmetrical Dual String Theories and their Field Theory Limits: A Review*, *Surveys High Energ. Phys.* **3** (1984) 127–160.
- [22] M. Fukugita and T. Yanagida, *Baryogenesis Without Grand Unification*, *Phys. Lett. B* **174** (1986) 45–47.
- [23] S. Davidson and A. Ibarra, *A Lower bound on the right-handed neutrino mass from leptogenesis*, *Phys. Lett. B* **535** (2002) 25–32, [[hep-ph/0202239](#)].
- [24] W. Buchmuller, P. Di Bari, and M. Plumacher, *Leptogenesis for pedestrians*, *Annals Phys.* **315** (2005) 305–351, [[hep-ph/0401240](#)].
- [25] S. Davidson, E. Nardi, and Y. Nir, *Leptogenesis*, *Phys. Rept.* **466** (2008) 105–177, [[arXiv:0802.2962](#)].
- [26] S. Weinberg, *Supersymmetry at Ordinary Energies. 1. Masses and Conservation Laws*, *Phys. Rev. D* **26** (1982) 287.
- [27] N. Sakai and T. Yanagida, *Proton Decay in a Class of Supersymmetric Grand Unified Models*, *Nucl. Phys. B* **197** (1982) 533.
- [28] S. W. Hawking, D. N. Page, and C. N. Pope, *THE PROPAGATION OF PARTICLES IN SPACE-TIME FOAM*, *Phys. Lett. B* **86** (1979) 175–178.
- [29] I. Antoniadis, J. R. Ellis, J. S. Hagelin, and D. V. Nanopoulos, *The Flipped $SU(5) \times U(1)$ String Model Revamped*, *Phys. Lett. B* **231** (1989) 65–74.
- [30] **Super-Kamiokande** Collaboration, A. Takenaka et al., *Search for proton decay via $p \rightarrow e^+\pi^0$ and $p \rightarrow \mu^+\pi^0$ with an enlarged fiducial volume in Super-Kamiokande I-IV*, *Phys. Rev. D* **102** (2020), no. 11 112011, [[arXiv:2010.16098](#)].
- [31] **DUNE** Collaboration, B. Abi et al., *Deep Underground Neutrino Experiment (DUNE), Far Detector Technical Design Report, Volume I Introduction to DUNE*, *JINST* **15** (2020), no. 08 T08008, [[arXiv:2002.02967](#)].
- [32] **DUNE** Collaboration, B. Abi et al., *Deep Underground Neutrino Experiment (DUNE), Far Detector Technical Design Report, Volume III: DUNE Far Detector Technical Coordination*, *JINST* **15** (2020), no. 08 T08009, [[arXiv:2002.03008](#)].
- [33] **DUNE** Collaboration, B. Abi et al., *Deep Underground Neutrino Experiment (DUNE), Far Detector Technical Design Report, Volume IV: Far Detector Single-phase Technology*, *JINST* **15** (2020), no. 08 T08010, [[arXiv:2002.03010](#)].
- [34] **DUNE** Collaboration, B. Abi et al., *Deep Underground Neutrino Experiment (DUNE), Far Detector Technical Design Report, Volume II: DUNE Physics*, [[arXiv:2002.03005](#)].
- [35] **JUNO** Collaboration, Z. Djurcic et al., *JUNO Conceptual Design Report*, [[arXiv:1508.07166](#)].
- [36] **JUNO** Collaboration, F. An et al., *Neutrino Physics with JUNO*, *J. Phys. G* **43** (2016), no. 3 030401, [[arXiv:1507.05613](#)].
- [37] **Hyper-Kamiokande** Collaboration, K. Abe et al., *Hyper-Kamiokande Design Report*, [[arXiv:1805.04163](#)].

- [38] K. Fridell, C. Hati, and V. Takhistov, *Non-Canonical Nucleon Decays as Window into Light New Physics*, [arXiv:2312.13740](#).
- [39] E. Gildener, *Gauge Symmetry Hierarchies*, *Phys. Rev. D* **14** (1976) 1667.
- [40] M. J. G. Veltman, *The Infrared - Ultraviolet Connection*, *Acta Phys. Polon. B* **12** (1981) 437.
- [41] R. Barbier et al., *R-parity violating supersymmetry*, *Phys. Rept.* **420** (2005) 1–202, [[hep-ph/0406039](#)].
- [42] G. R. Farrar and P. Fayet, *Phenomenology of the Production, Decay, and Detection of New Hadronic States Associated with Supersymmetry*, *Phys. Lett. B* **76** (1978) 575–579.
- [43] H. K. Dreiner, *An Introduction to explicit R-parity violation*, *Adv. Ser. Direct. High Energy Phys.* **21** (2010) 565–583, [[hep-ph/9707435](#)].
- [44] B. C. Allanach, A. Dedes, and H. K. Dreiner, *R parity violating minimal supergravity model*, *Phys. Rev. D* **69** (2004) 115002, [[hep-ph/0309196](#)]. [Erratum: *Phys.Rev.D* **72**, 079902 (2005)].
- [45] L. E. Ibanez and G. G. Ross, *Discrete gauge symmetries and the origin of baryon and lepton number conservation in supersymmetric versions of the standard model*, *Nucl. Phys. B* **368** (1992) 3–37.
- [46] H. K. Dreiner, C. Luhn, and M. Thormeier, *What is the discrete gauge symmetry of the MSSM?*, *Phys. Rev. D* **73** (2006) 075007, [[hep-ph/0512163](#)].
- [47] H. K. Dreiner, M. Hanussek, and C. Luhn, *What is the discrete gauge symmetry of the R-parity violating MSSM?*, *Phys. Rev. D* **86** (2012) 055012, [[arXiv:1206.6305](#)].
- [48] L. E. Ibanez and G. G. Ross, *Discrete gauge symmetry anomalies*, *Phys. Lett. B* **260** (1991) 291–295.
- [49] A. Y. Smirnov and F. Vissani, *Upper bound on all products of R-parity violating couplings lambda-prime and lambda-prime-prime from proton decay*, *Phys. Lett. B* **380** (1996) 317–323, [[hep-ph/9601387](#)].
- [50] E. Dudas, T. Gherghetta, K. Kaneta, Y. Mambrini, and K. A. Olive, *Limits on R-parity Violation in High Scale Supersymmetry*, *Phys. Rev. D* **100** (2019), no. 3 035004, [[arXiv:1905.09243](#)].
- [51] N. Chamoun, F. Domingo, and H. K. Dreiner, *Nucleon decay in the r-parity violating mssm*, *Phys. Rev. D* **104** (Jul, 2021) 015020.
- [52] I. Hinchliffe and T. Kaeding, *B+L violating couplings in the minimal supersymmetric Standard Model*, *Phys. Rev. D* **47** (1993) 279–284.
- [53] F. Vissani, *(B+L) conserving nucleon decays in supersymmetric models*, *Phys. Rev. D* **52** (1995) 4245–4247, [[hep-ph/9503227](#)].
- [54] L. J. Hall and M. Suzuki, *Explicit R-Parity Breaking in Supersymmetric Models*, *Nucl. Phys. B* **231** (1984) 419–444.
- [55] C. E. Carlson, P. Roy, and M. Sher, *New bounds on R-parity violating couplings*, *Phys. Lett. B* **357** (1995) 99–104, [[hep-ph/9506328](#)].
- [56] H. N. Long and P. B. Pal, *Nucleon instability in a supersymmetric SU(3) C x SU(3)-L x U(1) model*, *Mod. Phys. Lett. A* **13** (1998) 2355–2360, [[hep-ph/9711455](#)].

- [57] G. Bhattacharyya and P. B. Pal, *Upper bounds on all R-parity violating lambda lambda-prime-prime combinations from proton stability*, *Phys. Rev. D* **59** (1999) 097701, [[hep-ph/9809493](#)].
- [58] G. Bhattacharyya and P. B. Pal, *New constraints on R-parity violation from proton stability*, *Phys. Lett. B* **439** (1998) 81–84, [[hep-ph/9806214](#)].
- [59] D. Chang and W.-Y. Keung, *New limits on R-parity breakings in supersymmetric standard models*, *Phys. Lett. B* **389** (1996) 294–298, [[hep-ph/9608313](#)].
- [60] K. Choi, E. J. Chun, and J. S. Lee, *Proton decay with a light gravitino or axino*, *Phys. Rev. D* **55** (1997) 3924–3926, [[hep-ph/9611285](#)].
- [61] K. Choi, K. Hwang, and J. S. Lee, *Constraints on R-parity and B violating couplings in gauge mediated supersymmetry breaking models*, *Phys. Lett. B* **428** (1998) 129–135, [[hep-ph/9802323](#)].
- [62] D. Choudhury, H. K. Dreiner, P. Richardson, and S. Sarkar, *A Supersymmetric solution to the KARMEN time anomaly*, *Phys. Rev. D* **61** (2000) 095009, [[hep-ph/9911365](#)].
- [63] H. K. Dreiner, S. Heinemeyer, O. Kittel, U. Langenfeld, A. M. Weber, and G. Weiglein, *Mass Bounds on a Very Light Neutralino*, *Eur. Phys. J. C* **62** (2009) 547–572, [[arXiv:0901.3485](#)].
- [64] H. K. Dreiner, C. Hanhart, U. Langenfeld, and D. R. Phillips, *Supernovae and light neutralinos: SN1987A bounds on supersymmetry revisited*, *Phys. Rev. D* **68** (2003) 055004, [[hep-ph/0304289](#)].
- [65] H. K. Dreiner, J.-F. Fortin, J. Isern, and L. Ubaldi, *White Dwarfs constrain Dark Forces*, *Phys. Rev. D* **88** (2013) 043517, [[arXiv:1303.7232](#)].
- [66] J. de Vries, H. K. Dreiner, and D. Schmeier, *R-Parity Violation and Light Neutralinos at SHiP and the LHC*, *Phys. Rev. D* **94** (2016), no. 3 035006, [[arXiv:1511.07436](#)].
- [67] D. Dercks, J. De Vries, H. K. Dreiner, and Z. S. Wang, *R-parity Violation and Light Neutralinos at CODEX-b, FASER, and MATHUSLA*, *Phys. Rev. D* **99** (2019), no. 5 055039, [[arXiv:1810.03617](#)].
- [68] D. Dercks, H. K. Dreiner, M. Hirsch, and Z. S. Wang, *Long-Lived Fermions at AL3X*, *Phys. Rev. D* **99** (2019), no. 5 055020, [[arXiv:1811.01995](#)].
- [69] H. K. Dreiner, J. Y. Günther, and Z. S. Wang, *R-parity violation and light neutralinos at ANUBIS and MAPP*, *Phys. Rev. D* **103** (2021), no. 7 075013, [[arXiv:2008.07539](#)].
- [70] H. K. Dreiner, D. Köhler, S. Nangia, and Z. S. Wang, *Searching for a Single Photon from Lightest Neutralino Decays in R-parity-violating Supersymmetry at FASER*, [[arXiv:2207.05100](#)].
- [71] H. K. Dreiner, D. Köhler, S. Nangia, M. Schürmann, and Z. S. Wang, *Recasting bounds on long-lived heavy neutral leptons in terms of a light supersymmetric R-parity violating neutralino*, *JHEP* **08** (2023) 058, [[arXiv:2306.14700](#)].
- [72] J. Y. Günther, J. de Vries, H. K. Dreiner, Z. S. Wang, and G. Zhou, *Long-lived neutral fermions at the DUNE near detector*, *JHEP* **01** (2024) 108, [[arXiv:2310.12392](#)].
- [73] D. Curtin et al., *Long-Lived Particles at the Energy Frontier: The MATHUSLA Physics Case*, *Rept. Prog. Phys.* **82** (2019), no. 11 116201, [[arXiv:1806.07396](#)].

- [74] J. L. Feng et al., *The Forward Physics Facility at the High-Luminosity LHC*, *J. Phys. G* **50** (2023), no. 3 030501, [[arXiv:2203.05090](#)].
- [75] J. M. Berryman, A. de Gouvea, P. J. Fox, B. J. Kayser, K. J. Kelly, and J. L. Raaf, *Searches for Decays of New Particles in the DUNE Multi-Purpose Near Detector*, *JHEP* **02** (2020) 174, [[arXiv:1912.07622](#)].
- [76] L. Lee, C. Ohm, A. Soffer, and T.-T. Yu, *Collider Searches for Long-Lived Particles Beyond the Standard Model*, *Prog. Part. Nucl. Phys.* **106** (2019) 210–255, [[arXiv:1810.12602](#)].
- [77] A. Filimonova, R. Schäfer, and S. Westhoff, *Probing dark sectors with long-lived particles at BELLE II*, *Phys. Rev. D* **101** (2020), no. 9 095006, [[arXiv:1911.03490](#)].
- [78] J. Alimena et al., *Searching for long-lived particles beyond the Standard Model at the Large Hadron Collider*, *J. Phys. G* **47** (2020), no. 9 090501, [[arXiv:1903.04497](#)].
- [79] J. De Vries, H. K. Dreiner, J. Y. Günther, Z. S. Wang, and G. Zhou, *Long-lived Sterile Neutrinos at the LHC in Effective Field Theory*, *JHEP* **03** (2021) 148, [[arXiv:2010.07305](#)].
- [80] **Super-Kamiokande** Collaboration, K. Abe et al., *Search for proton decay via $p \rightarrow \nu K^+$ using 260 kiloton-year data of Super-Kamiokande*, *Phys. Rev. D* **90** (2014), no. 7 072005, [[arXiv:1408.1195](#)].
- [81] **Super-Kamiokande** Collaboration, Y. Fukuda et al., *The Super-Kamiokande detector*, *Nucl. Instrum. Meth. A* **501** (2003) 418–462.
- [82] H. K. Dreiner and M. Thormeier, *Supersymmetric Froggatt-Nielsen models with baryon and lepton number violation*, *Phys. Rev. D* **69** (2004) 053002, [[hep-ph/0305270](#)].
- [83] **JLQCD** Collaboration, S. Aoki et al., *Nucleon decay matrix elements from lattice QCD*, *Phys. Rev. D* **62** (2000) 014506, [[hep-lat/9911026](#)].
- [84] Y. Aoki, T. Izubuchi, E. Shintani, and A. Soni, *Improved lattice computation of proton decay matrix elements*, *Phys. Rev. D* **96** (2017), no. 1 014506, [[arXiv:1705.01338](#)].
- [85] J.-S. Yoo, Y. Aoki, P. Boyle, T. Izubuchi, A. Soni, and S. Syritsyn, *Proton decay matrix elements on the lattice at physical pion mass*, *Phys. Rev. D* **105** (2022), no. 7 074501, [[arXiv:2111.01608](#)].
- [86] F. Domingo and H. K. Dreiner, *Decays of a bino-like particle in the low-mass regime*, [[arXiv:2205.08141](#)].
- [87] H. K. Dreiner and G. G. Ross, *R-parity violation at hadron colliders*, *Nucl. Phys. B* **365** (1991) 597–613.
- [88] K. Agashe and M. Graesser, *R-parity violation in flavor changing neutral current processes and top quark decays*, *Phys. Rev. D* **54** (1996) 4445–4452, [[hep-ph/9510439](#)].
- [89] H. K. Dreiner, H. E. Haber, and S. P. Martin, *Two-component spinor techniques and Feynman rules for quantum field theory and supersymmetry*, *Phys. Rept.* **494** (2010) 1–196, [[arXiv:0812.1594](#)].
- [90] S. Dawson, *R-Parity Breaking in Supersymmetric Theories*, *Nucl. Phys. B* **261** (1985) 297–318.
- [91] H. E. Haber and D. Wyler, *RADIATIVE NEUTRALINO DECAY*, *Nucl. Phys. B* **323** (1989) 267–310.
- [92] **JUNO** Collaboration, A. Abusleme et al., *JUNO Sensitivity on Proton Decay $p \rightarrow \bar{\nu} K^+$ Searches*, [[arXiv:2212.08502](#)].

- [93] D. Stefan and A. M. Ankowski, *Nuclear effects in proton decay*, *Acta Phys. Polon. B* **40** (2009) 671–674, [[arXiv:0811.1892](#)].
- [94] O. Benhar, N. Farina, H. Nakamura, M. Sakuda, and R. Seki, *Electron- and neutrino-nucleus scattering in the impulse approximation regime*, *Phys. Rev. D* **72** (2005) 053005, [[hep-ph/0506116](#)].
- [95] A. M. Ankowski and J. T. Sobczyk, *Construction of spectral functions for medium-mass nuclei*, *Phys. Rev. C* **77** (2008) 044311, [[arXiv:0711.2031](#)].
- [96] H. W. Bertini, *Low-Energy Intranuclear Cascade Calculation*, *Phys. Rev.* **131** (1963) 1801–1821.
- [97] H. W. Bertini, *Intranuclear-cascade calculation of the secondary nucleon spectra from nucleon-nucleus interactions in the energy range 340 to 2900 mev and comparisons with experiment*, *Phys. Rev.* **188** (1969) 1711–1730.
- [98] H. W. Bertini and M. P. Guthrie, *News item results from medium-energy intranuclear-cascade calculation*, *Nucl. Phys. A* **169** (1971) 670–672.
- [99] **GEANT4** Collaboration, S. Agostinelli et al., *GEANT4—a simulation toolkit*, *Nucl. Instrum. Meth. A* **506** (2003) 250–303.
- [100] A. Heikkinen, N. Stepanov, and J. P. Wellisch, *Bertini intranuclear cascade implementation in GEANT4*, *eConf C0303241* (2003) MOMT008, [[nucl-th/0306008](#)].
- [101] T. M. Undagoitia, F. von Feilitzsch, M. Goger-Neff, C. Grieb, K. A. Hochmuth, L. Oberauer, W. Potzel, and M. Wurm, *Search for the proton decay $p \rightarrow K^+ \text{ anti-}\nu$ in the large liquid scintillator low energy neutrino astronomy detector LENA*, *Phys. Rev. D* **72** (2005) 075014, [[hep-ph/0511230](#)].
- [102] B. C. Allanach, A. Dedes, and H. K. Dreiner, *Bounds on R-parity violating couplings at the weak scale and at the GUT scale*, *Phys. Rev. D* **60** (1999) 075014, [[hep-ph/9906209](#)].
- [103] D. Dercks, H. Dreiner, M. E. Krauss, T. Opferkuch, and A. Reinert, *R-Parity Violation at the LHC*, *Eur. Phys. J. C* **77** (2017), no. 12 856, [[arXiv:1706.09418](#)].
- [104] **Super-Kamiokande** Collaboration, M. Litos et al., *Search for Dinucleon Decay into Kaons in Super-Kamiokande*, *Phys. Rev. Lett.* **112** (2014), no. 13 131803.
- [105] F. del Aguila, S. Bar-Shalom, A. Soni, and J. Wudka, *Heavy Majorana Neutrinos in the Effective Lagrangian Description: Application to Hadron Colliders*, *Phys. Lett. B* **670** (2009) 399–402, [[arXiv:0806.0876](#)].
- [106] Y. Liao and X.-D. Ma, *Operators up to Dimension Seven in Standard Model Effective Field Theory Extended with Sterile Neutrinos*, *Phys. Rev. D* **96** (2017), no. 1 015012, [[arXiv:1612.04527](#)].
- [107] I. Bischer and W. Rodejohann, *General neutrino interactions from an effective field theory perspective*, *Nucl. Phys. B* **947** (2019) 114746, [[arXiv:1905.08699](#)].